

**10) Response to Follow-up to Questions from the Sierra Club**

**Cole, Doug**

---

**From:** Jess Dervin-Ackerman <jess.dervin-ackerman@sierraclub.org>  
**Sent:** Tuesday, October 06, 2015 12:29 PM  
**To:** Cappio, Claudia; Schaaf, Libby; DL - City Council; Cole, Doug  
**Subject:** Articles and Research for Public Record: Coal Exports Public Hearing  
**Attachments:** grl25887-fig-0001\_10.1029%2F2009GL037950.pptx; Zhang -- transpacific transport of ozone -- 2008.pdf; Zhang -- Intercontinental source attribution of ozone -- 2009.pdf; PNAS 2014 Feb 111(5) 1736-41, Fig. 2.ppt; PNAS-2014-Lin-1736-41.pdf; Keep coal out of Oakland port - San Francisco Chronicle.pdf; Coal Free Oakland Letter to Mayor and Council 9.20.15.pdf; Coal Free Oakland Petition Signers10.5.15.xls; Assembly Join Resolution 35 Coal Exports.pdf

To Whom It May Concern,

Please consider the attached articles, research, policy, community sign on letter, and petition signers as part of the public record for the public hearing on coal through the Oakland Global Project.

Sincerely,

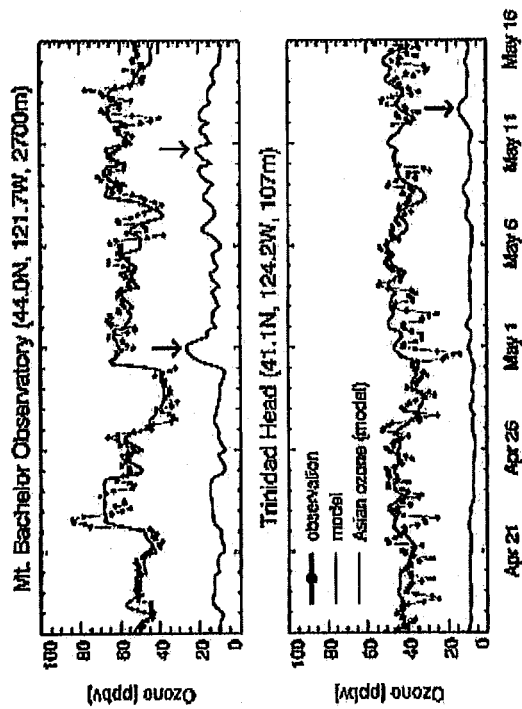
Jess Dervin-Ackerman

--  
Jess Dervin-Ackerman  
Conservation Manager

Sierra Club, San Francisco Bay Chapter  
2530 San Pablo Ave, Suite I  
Berkeley, CA 94702  
Office: (510) 848 - 0800 ext. 304  
Cell: (510) 693-7677  
[jess.dervin-ackerman@sierraclub.org](mailto:jess.dervin-ackerman@sierraclub.org)

The 5th annual David Brower Dinner is on October 22nd in San Francisco! This event brings together some of the region's most influential change-makers to honor local environmental heroes and the achievements of the Bay Chapter. Join us!  
*Tickets and sponsorships available [here](#).*

# Intercontinental source attribution of ozone pollution at western U.S. sites using an adjoint method



## Transpacific transport of ozone pollution and the effect of recent Asian emission increases on air quality in North America: an integrated analysis using satellite, aircraft, ozonesonde, and surface observations

L. Zhang<sup>1</sup>, D. J. Jacob<sup>1,2</sup>, K. F. Boersma<sup>2,\*</sup>, D. A. Jaffe<sup>3</sup>, J. R. Olson<sup>4</sup>, K. W. Bowman<sup>5</sup>, J. R. Worden<sup>5</sup>, A. M. Thompson<sup>6</sup>, M. A. Avery<sup>4</sup>, R. C. Cohen<sup>7</sup>, J. E. Dibb<sup>8</sup>, E. M. Flock<sup>9</sup>, H. E. Fuelberg<sup>10</sup>, L. G. Huey<sup>11</sup>, W. W. McMillan<sup>12</sup>, H. B. Singh<sup>13</sup>, and A. J. Weinheimer<sup>14</sup>

<sup>1</sup>Department of Earth and Planetary Sciences, Harvard University, Cambridge, MA 02138, USA

<sup>2</sup>School of Engineering and Applied Sciences, Harvard University, Cambridge, MA 02138, USA

<sup>3</sup>University of Washington, 18115 Campus Way NE, Bothell, WA 98021, USA

<sup>4</sup>Atmospheric Sciences Division, Langley Research Center, NASA, Hampton, VA 23681, USA

<sup>5</sup>Jet Propulsion Laboratory, California Institute of Technology, 4800 Oak Grove Drive, Pasadena, CA 91109, USA

<sup>6</sup>The Pennsylvania State University, Department of Meteorology, 503 Walker Building, University Park, PA 16802-5013 USA

<sup>7</sup>Department of Chemistry, University of California, Berkeley, CA 94720, USA

<sup>8</sup>University of New Hampshire, Climate Change Research Center, 39 College Road, Durham, NH 03824, USA

<sup>9</sup>Earth Observing Laboratory, National Center for Atmospheric Research, Boulder, CO 80307, USA

<sup>10</sup>Department of Meteorology, Florida State University, Tallahassee, FL 32306-4520, USA

<sup>11</sup>School of Earth and Atmospheric Sciences, Georgia Institute of Technology, Atlanta, GA 30332-0340, USA

<sup>12</sup>Department of Physics, University of Maryland Baltimore County, 1000 Hilltop Circle, Baltimore, MD 21250, USA

<sup>13</sup>NASA Ames Research Center, MS-245-5, Moffett Field, CA 94035, USA

<sup>14</sup>National Center for Atmospheric Research, 1850 Table Mesa Drive, Boulder, CO 80305, USA

\*now at: KNMI, PO Box 201, 3730 AE De Bilt, The Netherlands

Received: 26 March 2008 – Published in Atmos. Chem. Phys. Discuss.: 24 April 2008

Revised: 1 August 2008 – Accepted: 11 September 2008 – Published: 22 October 2008

**Abstract.** We use an ensemble of aircraft, satellite, sonde, and surface observations for April–May 2006 (NASA/INTEX-B aircraft campaign) to better understand the mechanisms for transpacific ozone pollution and its implications for North American air quality. The observations are interpreted with a global 3-D chemical transport model (GEOS-Chem). OMI NO<sub>2</sub> satellite observations constrain Asian anthropogenic NO<sub>x</sub> emissions and indicate a factor of 2 increase from 2000 to 2006 in China. Satellite observations of CO from AIRS and TES indicate two major events of Asian transpacific pollution during INTEX-B. Correlation between TES CO and ozone observations shows evidence

for transpacific ozone pollution. The semi-permanent Pacific High and Aleutian Low cause splitting of transpacific pollution plumes over the Northeast Pacific. The northern branch circulates around the Aleutian Low and has little impact on North America. The southern branch circulates around the Pacific High and some of that air impacts western North America. Both aircraft measurements and model results show sustained ozone production driven by peroxyacetyl/nitrate (PAN) decomposition in the southern branch, roughly doubling the transpacific influence from ozone produced in the Asian boundary layer. Model simulation of ozone observations at Mt. Bachelor Observatory in Oregon (2.7 km altitude) indicates a mean Asian ozone pollution contribution of 9±3 ppbv to the mean observed concentration of 54 ppbv, reflecting mostly an enhancement in background ozone rather



Correspondence to: L. Zhang  
(linzhang@fas.harvard.edu)

than episodic Asian plumes. Asian pollution enhanced surface ozone concentrations by 5–7 ppbv over western North America in spring 2006. The 2000–2006 rise in Asian anthropogenic emissions increased this influence by 1–2 ppbv.

## 1 Introduction

Rapid industrial development in eastern Asia and specifically in China has resulted in unprecedented growth in  $\text{NO}_x$  emissions with implications for both regional and global tropospheric ozone (Wild and Akimoto, 2001). Efforts to improve US air quality through domestic emission controls could be partly compromised by Asian industrialization and the associated transpacific transport of pollution (Jacob et al., 1999; Fiore et al., 2002). Better understanding the impact of rising Asian  $\text{NO}_x$  emissions on transpacific ozone pollution and surface ozone air quality in the United States is therefore of great interest. We address this issue here through a global 3-D model analysis of observations from the NASA Intercontinental Chemical Transport Experiment – Phase B (INTEX-B) aircraft campaign, conducted in spring 2006 over the Northeast Pacific. We integrate into our analysis concurrent measurements from ground sites, sondes, and satellites.

Ozone is produced in the troposphere by the photochemical oxidation of CO and volatile organic compounds (VOCs) in the presence of nitrogen oxides ( $\text{NO}_x \equiv \text{NO} + \text{NO}_2$ ). On a global scale, the photochemical production of ozone dominates over the stratospheric influx (Prather and Ehhalt, 2001; Sudo and Akimoto, 2007), and is limited mostly by the supply of  $\text{NO}_x$  and methane (Wang et al., 1998b). Anthropogenic sources of  $\text{NO}_x$  from combustion combined with the global rise in methane have probably doubled the tropospheric ozone burden in the northern hemisphere over the past century (Prather and Ehhalt, 2001). Ozone has a lifetime of days in the continental boundary layer but weeks in the free troposphere (Jacob et al., 1996; Thompson et al., 1996; Wang et al., 1998b; Fiore et al., 2002), and thus can affect continents downwind.

The dependence of ozone production on  $\text{NO}_x$  is highly nonlinear; the ozone production efficiency (OPE) per unit  $\text{NO}_x$  consumed increases rapidly as the  $\text{NO}_x$  concentration decreases (Liu et al., 1987). Ozone production within the continental boundary layer is relatively inefficient because of the high- $\text{NO}_x$  conditions. A small fraction of emitted  $\text{NO}_x$  exported to the free troposphere by frontal lifting, deep convection, or boundary layer venting can lead to disproportionately large ozone production in the free troposphere over the continent and downwind (Jacob et al., 1993; Thompson et al., 1994). The peroxyacetylnitrate (PAN) reservoir for  $\text{NO}_x$  can be vented from the boundary layer and transported on a global scale at cold temperatures, eventually decomposing to release  $\text{NO}_x$  in the remote troposphere as air masses subside and producing ozone with very high efficiency. Previ-

ous studies using aircraft measurements from the PHOBEA, TRACE-P, and ITCT-2K2 campaigns (Kotchenruther et al., 2001; Heald et al., 2003; Hudman et al., 2004) found that PAN decomposition may represent a dominant component of the ozone enhancement in transpacific Asian pollution plumes. The INTEX-B campaign offers far more geographical coverage over the Northeast Pacific and we will see that it enables a better understanding of the mechanisms of ozone production in transpacific plumes.

Asian pollution is typically exported to the Pacific by frontal lifting in warm conveyor belts (WCBs), convection, and orographic lifting (Liu et al., 2003; Brock et al., 2004; Liang et al., 2004; Kiley et al., 2006; Dickerson et al., 2007). It can then be transported across the Pacific in 5–10 days in the free troposphere (Yienger et al., 2000; Jaffe et al., 2001; Stohl et al., 2002). The mean transport time to the surface of western North America is of the order of 2–3 weeks (Liu and Mauzerall, 2005). The transport is most rapid and frequent in spring due to active cyclonic activity and strong westerly winds (Forster et al., 2004; Liang et al., 2004). While Asian plumes with correlated CO and ozone are often observed in the free troposphere and at mountain sites over the western United States (Price et al., 2004; Jaffe et al., 2005; Weiss-Penzias et al., 2007), no such plumes are observed at the surface for ozone (Goldstein et al., 2004), presumably because of dilution during entrainment into the boundary layer (Hudman et al., 2004). Asian ozone pollution in US surface air thus mostly reflects an increase in background concentrations (Fiore et al., 2003). Background ozone levels in air entering western North America have increased approximately 10 ppbv between 1984 and 2002 (Jaffe et al., 2003) and ozone concentrations across the western United States show a significant increase with a mean trend of  $0.26 \text{ ppbv a}^{-1}$  (Jaffe and Ray, 2007). The cause for this increase is not clear but rising Asian emissions may be a contributing source.

A unique feature of the INTEX-B campaign was the availability of extensive satellite observations of tropospheric ozone,  $\text{NO}_2$ , and CO to complement the aircraft observations. Satellites provide a growing resource to quantify emissions of ozone precursors (Martin et al., 2006) and to map the transpacific transport of pollutants (Heald et al., 2003, 2006). They greatly expand the temporal and spatial scale of in situ measurements but are limited in precision, vertical resolution, and the number of species observed. Aircraft vertical profiles during INTEX-B provided validation data for the OMI ( $\text{NO}_2$ ), AIRS (CO), and TES (ozone, CO) satellite sensors (Boersma et al., 2008; Luo et al., 2007b; Richards et al., 2008). Here we use these satellite observations to constrain Asian  $\text{NO}_x$  emissions ( $\text{NO}_2$  from OMI), track transpacific plumes (CO from AIRS as a long-lived pollution tracer), and observe ozone production in transpacific Asian plumes (ozone and CO from TES). We examine the consistency between the satellite and aircraft information and apply the aircraft data to further analysis of plume chemistry. We also use sonde data from INTEX Ozonesonde Network

Study (IONS) (Thompson et al., 2008) to test model results, and use ground-based measurements at Mount Bachelor Observatory in central Oregon (Jaffe et al., 2005; Reidmiller et al., 2008) to link observed Asian pollution influences in the free troposphere to North American surface air quality.

## 2 Observations and model

### 2.1 In-situ measurements

The NASA INTEX-B aircraft mission took place from 17 April to 15 May 2006 over the Northeast Pacific and the west coast of North America (Singh et al., 2008<sup>1</sup>). It used the NASA DC-8 (ceiling 12 km) as its primary platform operating out of Honolulu and Anchorage, complemented with the NSF/NCAR C-130 (ceiling 7 km) operating out of Seattle. Figure 1 shows the flight tracks of the DC-8 and C-130 aircraft. These included extensive vertical profiling on all flights. The DC-8 conducted 10 science flights of about 9-h duration each, with large latitudinal coverage over the Northeast Pacific. The C-130 conducted 12 science flights of about 8-h duration each off and over the US Northwest Coast. Quasi-Lagrangian sampling studies were performed between the DC-8 and the C-130 to track the chemical evolution of Asian pollution plumes (Latto and Fuelberg, 2007).

Details of the chemical payload on both aircraft are given by Singh et al. (in preparation). We principally make use here of the 1-min average measurements of ozone, CO, NO, NO<sub>2</sub>, PAN, OH, and HO<sub>2</sub>. Intercomparisons between the two aircraft show excellent agreement for ozone, CO, and NO<sub>x</sub>, but for PAN the correlation is poor and C-130 measurements are 23% higher than DC-8 on average as discussed in Chen et al. (2007).

Additional in situ data for the INTEX-B period analyzed in our study include ozonesonde observations at Trinidad Head (California) and Richland (Washington) made during the IONS-06 collaborative field campaign (Thompson et al., 2008; <http://eroc.gsfc.nasa.gov/intexb/ions06.html>), and surface measurements at Mount Bachelor Observatory (MBO, 44.0° N, 121.7° W, 2.7 km altitude in Oregon) (Wolfe et al., 2007; Reidmiller et al., 2008).

### 2.2 Satellites

We use satellite observations from OMI and TES aboard Aura and AIRS aboard Aqua. Aura was launched in July 2004 into a polar, sun-synchronous orbit with ascending equator crossing around 1345 local time. The Ozone Monitoring Instrument (OMI) is a nadir-scanning instrument

<sup>1</sup>Singh, H. B., Brune, W. H., Crawford, J. H., Jacob, D. J., Russell, P. B., et al.: Chemistry and Transport of Pollution over the Gulf of Mexico and the Pacific: Spring 2006 INTEX-B Campaign Overview and First Results, *Atmos. Chem. Phys.*, submitted, 2008.

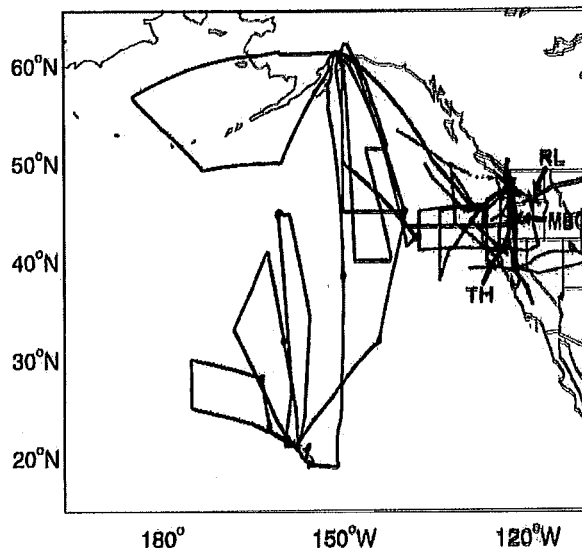


Fig. 1. Flight tracks of the NASA DC-8 (black) and NSF/NCAR C-130 (red) aircraft during the INTEX-B campaign (17 April–15 May 2006). The green stars show the locations of the Mt. Bachelor Observatory (MBO) in Oregon (2.7 km altitude), Trinidad Head (TH) in California, and Richland (RL) in Washington.

which measures backscattered solar radiation over the 270–500 nm wavelength range with a spectral resolution of 0.42–0.63 nm (Levelt et al., 2006). It has a spatial resolution of 13×24 km<sup>2</sup> at nadir and daily global coverage. We use here near-real time (NRT) tropospheric NO<sub>2</sub> columns retrieved by KNMI/NASA (Boersma et al., 2007). This product was successfully validated with DC-8 NO<sub>2</sub> vertical profiles (Boersma et al., 2008).

The Tropospheric Emission Spectrometer (TES) is a Fourier transform IR emission spectrometer with high spectral resolution (0.1 cm<sup>-1</sup> apodized) and a wide spectral range (650–3050 cm<sup>-1</sup>), enabling retrieval of both tropospheric ozone and CO in the nadir based on optimal estimation techniques (Beer et al., 2006; Bowman et al., 2006). Joint retrieval of ozone and CO enables TES to diagnose ozone pollution influences through O<sub>3</sub>-CO correlations (Zhang et al., 2006). During INTEX-B, TES alternated daily between “global survey” and “step-and-stare” observational modes. The standard products (“global surveys”) consist of 16 daily orbits across the North Pacific with retrievals spaced 1.6° along the orbit track. The “step-and-stare” observations have denser nadir coverage along the orbit track over the North Pacific. Vertical profiles retrieved from TES provide 1–2 degrees of freedom for signal (DOFS) for ozone in the troposphere corresponding to about 6 km vertical resolution, and about 1 DOFS for CO weighted towards the middle troposphere (Worden et al., 2004). We use V002 of TES data. Validation with ozonesondes and INTEX-B aircraft data shows that TES ozone profiles are biased high by 3–10 ppbv (Nassar

et al., 2008; Richards et al., 2008). TES CO measurements are consistent with those from MOPITT (Luo et al., 2007a) and within  $\pm 15\%$  of the INTEX-B aircraft data (Luo et al., 2007b). We filter out retrievals with poor sensitivity (diagonal term of the averaging kernel matrix at 681 hPa  $< 0.01$ , corresponding to  $< 0.25$  DOFS (Luo et al., 2007a)). To ensure that our conclusions are not affected by the variable a priori used to regularize the TES retrievals, we reprocess the TES profiles using a fixed a priori following Zhang et al. (2006).

The Atmospheric Infrared Sounder (AIRS) was launched on the NASA Aqua satellite in May 2002. It is a cross-track scanning grating spectrometer covering the 3.7 to 16  $\mu\text{m}$  spectral range with 2378 channels (Aumann et al., 2003). AIRS has a spatial resolution of 45 km at nadir and a 1650 km cross-track swath, enabling daily global coverage. CO retrievals are obtained at 4.7  $\mu\text{m}$  including for partly cloudy scenes (McMillan et al., 2005). We use version 4.2 of AIRS CO retrievals (McMillan et al., 2008). AIRS shows a positive bias of 15–20 ppbv relative to MOPITT over the oceans (Warner et al., 2007). Here we use AIRS observations of CO column qualitatively due to lack of well-defined averaging kernels in version 4.2.

### 2.3 Model description

We use the GEOS-Chem global 3-D model of tropospheric chemistry (v7-04-09; <http://www.as.harvard.edu/chemistry/trop/geos/>) driven by GEOS-4 assimilated meteorological observations from the NASA Global Modeling and Assimilation Office (GMAO). The model is applied to a global simulation of ozone- $\text{NO}_x$ -VOC-aerosol chemistry. General descriptions of GEOS-Chem are given by Bey et al. (2001) and Park et al. (2004), and previous applications to transpacific ozone chemistry include studies by Fiore et al. (2002), Jaeglé et al. (2003), Weiss-Penzias et al. (2004), Bertsch et al. (2004), Goldstein et al. (2004), Hudman et al. (2004), and Liang et al. (2007).

Meteorological fields in the GEOS-4 data have a temporal resolution of 6 h (3 h for surface variables and mixing depths) and a horizontal resolution of  $1^\circ$  latitude by  $1.25^\circ$  longitude, with 55 levels in the vertical. We degrade the horizontal resolution to  $2^\circ$  latitude by  $2.5^\circ$  longitude for input to GEOS-Chem. The simulations are conducted for April–May 2006 at  $2^\circ \times 2.5^\circ$  resolution. They are initialized on 1 April 2006 with GEOS-Chem fields generated by an 8-month spin-up simulation with  $4^\circ \times 5^\circ$  resolution.

Zhang et al.<sup>2</sup> ([http://www.cgrer.uiowa.edu/EMISSION\\_DATA\\_new/index\\_16.html](http://www.cgrer.uiowa.edu/EMISSION_DATA_new/index_16.html)) compiled a detailed anthropogenic emission inventory for Asia ( $8^\circ\text{N}$ – $50^\circ\text{N}$ ,  $80^\circ\text{E}$ – $150^\circ\text{E}$ ) for the spring 2006 period of INTEX-B (hereafter

referred to as S2006). We use their emission estimates except for  $\text{NO}_x$  which we derive instead from OMI  $\text{NO}_2$  data as a better estimate (Sect. 3). For US anthropogenic emissions we use the National Emission Inventory for 1999 (NEI 99) from the US Environmental Protection Agency (EPA) (<http://www.epa.gov/ttn/chieffnet/>). For the rest of the world we use anthropogenic emissions from the Global Emission Inventory Activity (GEIA), scaled to 1998 on the basis of national energy statistics as described by Bey et al. (2001).

Streets et al. (2003) previously reported an anthropogenic emission inventory for Asia in 2000 (hereafter referred to as S2000), and we will use that inventory in a sensitivity simulation to assess the impact of rising Asian emissions from 2000 to 2006. For the same Asian region, the S2006 inventory is 41% higher for CO, 45% higher for non-methane VOCs (NMVOCs), and 65% higher for  $\text{NO}_x$ . Our  $\text{NO}_x$  source constrained by the OMI  $\text{NO}_2$  observations is 2 times higher than S2000. Some of the change in the CO inventory in S2006 relative to S2000 reflects an underestimate in the original inventory (Streets et al., 2006), in addition to emission growth. The increase in NMVOCs reflects emission growth and is consistent with Ohara et al. (2007). The increase in  $\text{NO}_x$  also mainly reflects emission growth, as will be discussed in Sect. 3.

Biomass burning emissions are from a monthly climatological inventory (Duncan et al., 2003). Fire emissions over Southeast Asia in 2006 were not unusual compared with previous years (van der Werf et al., 2006; <http://ess1.ess.uci.edu/~jranders>). Soil  $\text{NO}_x$  emissions are computed using a modified version of the algorithm by Yienger and Levy (1995) with canopy reduction factors described by Wang et al. (1998a). Emissions of  $\text{NO}_x$  from lightning are linked to deep convection following the parameterization of Price and Rind (1992) with vertical profiles taken from Pickering et al. (1998). Following the suggestions by Martin et al. (2006) and Hudman et al. (2007) and evidence from observations (Huntrieser et al., 2006), we use a  $\text{NO}_x$  yield per flash of 125 moles in the tropics and 500 moles at northern mid-latitudes (north of  $30^\circ\text{N}$ ). The resulting lightning source is  $6\text{ Tg N a}^{-1}$  globally including  $1.6\text{ Tg N a}^{-1}$  north of  $30^\circ\text{N}$ . Transport of ozone from the stratosphere is simulated using the “Synoz” boundary condition of McLinden et al. (2000), which imposes a global cross-tropopause ozone flux of approximately  $495\text{ Tg ozone a}^{-1}$  transported downward by the model.

We present results from three full-chemistry simulations: (1) the standard simulation for 2006 as described above; (2) a sensitivity simulation without Asian ( $8^\circ$ – $50^\circ\text{N}$ ,  $80^\circ$ – $150^\circ\text{E}$ ) anthropogenic emissions (fossil fuel+biofuel), which allows us to derive Asian pollution enhancements in the standard simulation by difference; and (3) a sensitivity simulation for 2000 using S2000 Asian emissions from Streets et al. (2003) to derive the effect of 2000–2006 regional growth in emissions. We also conduct single-tracer simulations of odd oxygen ( $\text{O}_x \equiv \text{O}_3 + \text{NO}_2 + 2\text{NO}_3 + 3\text{N}_2\text{O}_5 + \text{HNO}_3 + \text{HNO}_4$

<sup>2</sup>Zhang, Q., Streets, D. G., He, K., et al.: A new inventory of anthropogenic emissions in Asia for the year 2005/2006, Atmos. Chem. Phys., manuscript in preparation, 2008.

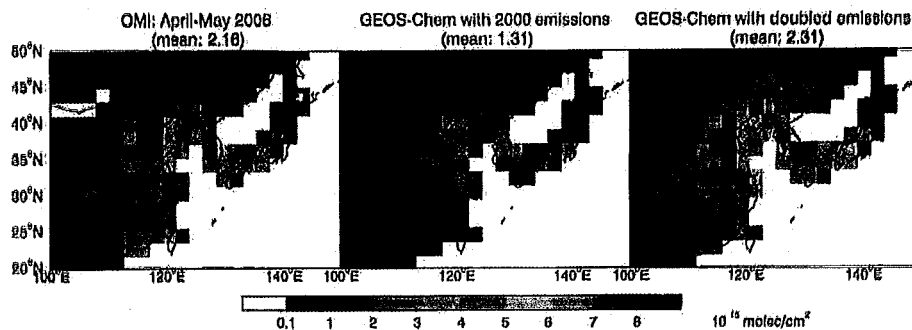


Fig. 2. Mean tropospheric  $\text{NO}_2$  columns from OMI and the GEOS-Chem model in April–May 2006 over eastern Asia. The OMI data (left panel) have been mapped on the  $2^\circ \times 2.5^\circ$  GEOS-Chem grid. GEOS-Chem model results are shown using 2000 anthropogenic  $\text{NO}_x$  emissions from Streets et al. (2003) (central panel) and a doubling of these emissions to represent 2006 conditions (right panel). The numbers in parentheses are the mean column values over eastern Asia.

peroxyacetyl nitrates), using archived 3-D fields of daily production rates and loss frequencies from the above simulations. This ozone tracer technique has been applied in a number of model studies to track the transport and fate of ozone produced in different regions (Wang et al., 1998b; Li et al., 2002; Sudo and Akimoto, 2007). We use it here to assess the relative contributions to transpacific ozone pollution from ozone produced in the Asian boundary layer versus formed downwind of Asia following  $\text{NO}_x$  and PAN export.

### 3 Constraints on Asian anthropogenic $\text{NO}_x$ emissions

The bottom-up combustion inventories for developing countries such as China are subject to large errors in available energy statistics and emission factors (Streets et al., 2003). We use here OMI tropospheric  $\text{NO}_2$  columns to provide top-down constraints on surface  $\text{NO}_x$  emissions for April–May 2006 over eastern Asia ( $20^\circ$ – $50^\circ$  N,  $100^\circ$ – $150^\circ$  E) including East China, Japan, and Korea. Following Martin et al. (2003), we determine local top-down surface  $\text{NO}_x$  emissions from the OMI  $\text{NO}_2$  columns by applying the GEOS-Chem relationship between  $\text{NO}_2$  columns and local emissions derived from the bottom-up inventory and sampled close to the satellite overpass time. We adopt the improvement from Wang et al. (2007) by accounting for contributions from external and non-surface sources, including in particular lightning and biomass burning in Southeast Asia. Contributions from these sources to tropospheric  $\text{NO}_2$  columns over eastern Asia were identified by GEOS-Chem sensitivity simulations with anthropogenic emissions over eastern Asia shut off. They typically represent 10–20%.

Figure 2 shows the  $\text{NO}_2$  tropospheric columns observed by OMI (left panel) vs. simulated by GEOS-Chem using S2000 anthropogenic  $\text{NO}_x$  emissions from Streets et al. (2003) (central panel) at the satellite overpass time. The model is 40% too low. We can match the OMI data by doubling

the S2000 anthropogenic  $\text{NO}_x$  emissions over eastern Asia (including China, Japan, and Korea), as shown in the right panel. This yields a high spatial correlation with OMI observations ( $r=0.92$ ,  $n=209$  on the  $2^\circ \times 2.5^\circ$  grid) as well as negligible bias (slope of 0.94 for the reduced-major-axis regression line). Walker et al.<sup>3</sup> obtained a similar constraint on Asian  $\text{NO}_x$  emissions using SCIAMACHY satellite  $\text{NO}_2$  data.

Our factor of 2 correction to the S2000 inventory likely reflects actual 2000–2006 emission growth in China and underestimation of bottom-up estimates for Japan and Korea. The S2006 bottom-up inventory (Zhang et al., in preparation) for the INTEX-B period shows a 98% growth of  $\text{NO}_x$  anthropogenic emissions from China relative to S2000, in close agreement with our results. Wang et al. (2007) previously found the S2000 inventory to be 15% lower than contemporary top-down constraints from the GOME  $\text{NO}_2$  satellite instrument. It thus appears that Chinese anthropogenic  $\text{NO}_x$  emissions have indeed doubled from 2000 to 2006. Previous trend analyses of Chinese anthropogenic  $\text{NO}_x$  emissions for the 1996–2004 period indicated an accelerating growth rate, with total growth for that period of 61% in the bottom-up inventory (Zhang et al., 2007) and 95% from satellite data (van der A et al., 2006).

The top-down constraints from OMI also imply factor of 2 increases in Japan and South Korean emissions relative to the S2000 inventory. However, S2006 report no significant 2000–2006 emission changes in these regions. Bottom-up and top-down analyses for earlier periods also show little trend (Richter et al., 2005; Ohara et al., 2007). The correction to the S2000 inventory in Japan and Korea needed to match the OMI data in Fig. 2 thus appears to reflect an underestimate in the inventory rather than an actual 2000–2006 emission trend. Jaeglé et al. (2005) and Wang et al. (2007)

<sup>3</sup>Walker, T. W., Martin, R. V., van Donkelaar, A., et al.: Transpacific transport of reactive nitrogen and ozone during spring, manuscript in preparation, 2008.

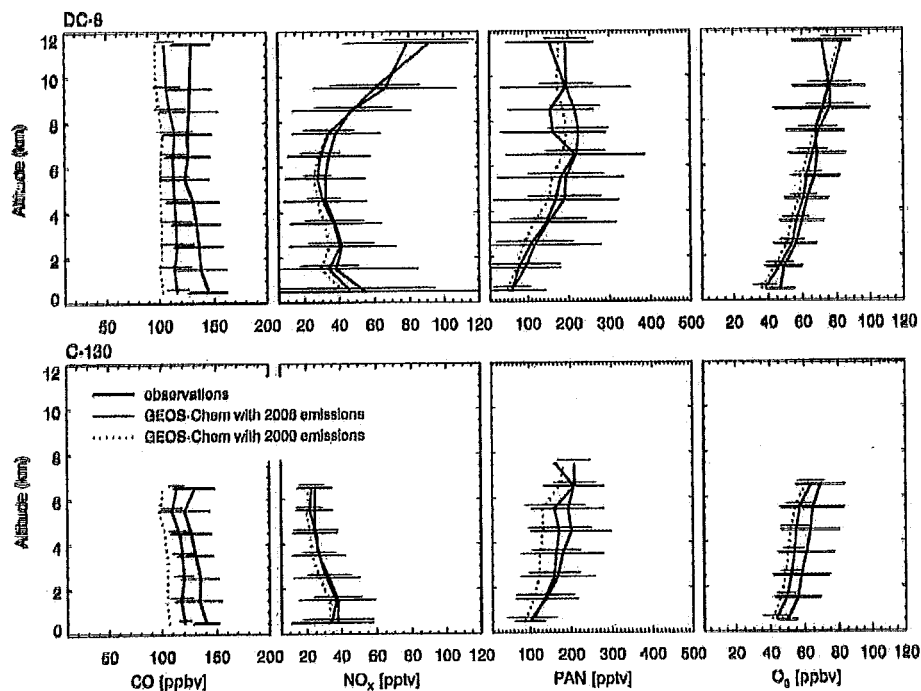


Fig. 3. Mean vertical profiles of CO, NO<sub>x</sub>, PAN, and O<sub>3</sub> concentrations over the Northeast Pacific during INTEX-B (April–May 2006). Observations (black) from the DC-8 (top) and C-130 (bottom) aircraft are compared to GEOS-Chem model results with 2006 Asian emissions (red solid) and 2000 Asian emissions (red dash). Horizontal bars are standard deviations. Here and in subsequent figures, the observations have been filtered to remove urban plumes, biomass burning plumes, and stratospheric air as described in the text. Model results are sampled along the flight tracks at the time of the flights, and observations are averaged over the model grid.

previously indicated a 30%–50% underestimate in the S2000 inventory relative to GOME NO<sub>2</sub> observations over Japan.

In what follows, we will interpret the doubling of anthropogenic NO<sub>x</sub> emissions in eastern Asia relative to S2000 as representing the actual 2000–2006 regional growth rate in emissions. This interpretation overestimates the actual growth by about 30% due to the apparent underestimation in S2000 for Japan and Korea. In any case, our standard simulation for 2006 includes our best estimate of East Asian emissions for that year constrained by the OMI data.

#### 4 Mean vertical profiles

We compare in Fig. 3 the observed and simulated mean vertical distributions of CO, NO<sub>x</sub>, PAN, and ozone concentrations for the ensemble of DC-8 and C-130 flights in Fig. 1. Model results are sampled along the flight tracks at the time of flights. Observations are gridded to model resolution. The comparison excludes urban plumes observed during take-off and landing as diagnosed by NO<sub>2</sub> > 500 pptv and altitude < 3 km; biomass burning plumes as diagnosed by HCN > 500 pptv or CH<sub>3</sub>CN > 225 pptv; and stratospheric air as diagnosed by O<sub>3</sub>/CO > 1.25 mol mol<sup>-1</sup>. These filters exclude 1%, 4% (urban plumes); 5%, 4% (biomass burning plumes);

and 7%, 0% (stratospheric air) of the data for the DC-8 and C-130, respectively. The stratospheric filter does not exclude stratospheric influence within the troposphere, as mixing of stratospheric and tropospheric air masses causes the O<sub>3</sub>/CO ratio to drop rapidly below the filter threshold.

CO profiles show little mean vertical structure. Modeled CO is 15% lower than observations, consistent with an OH overestimate in the model. Figure 4 shows the mean simulated vs. observed vertical distributions of OH and HO<sub>2</sub> concentrations. The model is too high for OH by 27% on average in the DC-8 data and by a comparable factor in the C-130 data. In contrast there is no significant bias for HO<sub>2</sub>. Ren et al. (2007) found that the OH and HO<sub>2</sub> observations from the DC-8 aircraft are within 15% of calculations from the NASA Langley photochemical box model (Olson et al. 2006) constrained with the ensemble of concurrent aircraft observations. To investigate this discrepancy, we conducted a test where we constrained the NASA Langley box model with GEOS-Chem output rather than observations from the DC-8 aircraft. This closely reproduced the OH and HO<sub>2</sub> concentrations simulated by GEOS-Chem, indicating that differences in chemical mechanisms are not responsible for the discrepancy. It appears instead that the discrepancy is mostly caused by an overestimate of water vapor in the GEOS-4 data set and

upper tropospheric NO concentrations in GEOS-Chem relative to the observations.

Observations of NO and NO<sub>2</sub> from both the DC-8 and the C-130 are in photostationary state and the absolute values are in agreement with the GEOS-Chem simulation at low altitude (below 6 km for the DC-8 and below 4 km for the C-130). At higher altitudes the NO/NO<sub>2</sub> ratio from both platforms is inconsistent with the assumption of photostationary state. Differences for the C-130 data are within the uncertainty in the instrument zero offsets (<5 pptv). For the DC-8 the differences become larger than that can be explained as uncertainties in the measurements above 8 km. The GEOS-Chem model overestimates NO measurements from DC-8 by 50% at 10 km (60 vs. 40 pptv) and underestimates NO<sub>2</sub> at the same altitude by a factor of 2 (20 vs. 40 pptv). By coincidence NO<sub>x</sub> is in agreement. If we attribute all of the error to one or the other measurement, then the GEOS-Chem model predicts either 50% too much NO<sub>x</sub> or 100% too little at 10 km. Here and in what follows we use total NO<sub>x</sub> as the comparison metric.

Comparisons of simulated and observed NO<sub>x</sub> and PAN in Fig. 3 show a low bias in the model with 2000 Asian emissions, which largely disappears in the model with 2006 Asian emissions. The doubling of anthropogenic NO<sub>x</sub> emissions over eastern Asia from 2000 to 2006 increases NO<sub>x</sub> concentrations by 3 pptv over the Northeast Pacific in the model. The PAN simulation with 2006 Asian emissions shows a 14% overestimate relative to the DC-8 observations while a 6% underestimate relative to C-130 observations, consistent with the 23% systematic difference in PAN measurements between the two aircraft (Chen et al., 2007). The 2000–2006 rise in Asian anthropogenic emissions increases the mean simulated PAN concentrations by 26 pptv (21%). Jaffe et al. (2007) compared the INTEX-B C-130 aircraft observations of NO<sub>x</sub> and PAN to their previous observations from the PHOBEA aircraft campaign in 1999 over the Northwest Coast of the United States, and found no significant change in NO<sub>x</sub> but a 22% mean increase in PAN.

Model results for ozone in Fig. 3 show a 3 ppbv mean increase from the 2000–2006 rise in Asian anthropogenic emissions. The model result with 2006 Asian emissions is consistent with DC-8 measurements. Comparison with C-130 measurements shows a negative bias of 5 ppbv. The DC-8 aircraft covered a large region over the Northeast Pacific, while the C-130 flew over the North American West Coast (Fig. 1), where stratospheric influence on ozone is particularly strong in spring (Cooper et al., 2004). Hudman et al. (2004) previously found that GEOS-Chem underestimated observed ozone concentrations from the ITCT 2K2 campaign over California in April–May 2002 by up to 10 ppbv due to its failure to reproduce high-ozone layers of stratospheric origin.

We further compared model results with sonde measurements from IONS-06. Figure 5 shows the comparison with the mean ozonesonde profiles at Trinidad Head on the

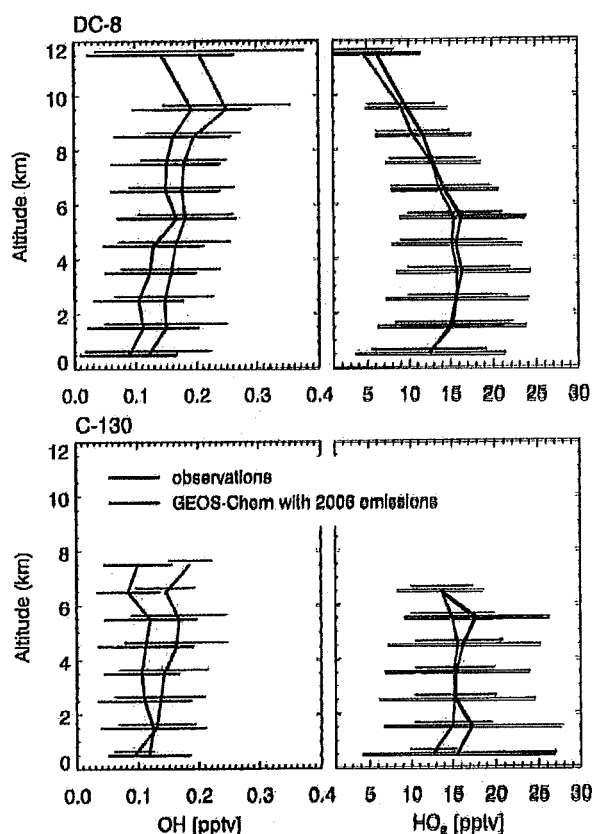


Fig. 4. Same as Fig. 3 but for OH and HO<sub>2</sub>. Only model results with 2006 Asian emissions are shown.

northern California coast (41° N, 124° W) and Richland in Washington (46° N, 119° W) during the INTEX-B period. The model reproduces the mean observed ozone profile at Trinidad Head but is 5 ppbv too low at 2–5 km. At Richland where stratospheric influences are more pronounced, the model is 10 ppbv too low in the free troposphere. Similar GEOS-Chem underestimate of the ozonesonde observations at Trinidad Head was reported by Hudman et al. (2004) for the ITCT-2K2 aircraft campaign.

## 5 Satellite and aircraft observations of transpacific transport

### 5.1 Transpacific transport as seen from satellites

Figure 6 shows AIRS (CO) and TES (CO, ozone) time series for the INTEX-B period over the Northwest and Northeast Pacific. AIRS has daily global coverage while TES is much sparser. AIRS observations of CO column over the Northwest Pacific show Asian outflow events every 3–6 days. These outflow events are associated with the passage of cold fronts across the Asian Pacific Rim (Liu et al., 2003; Heald

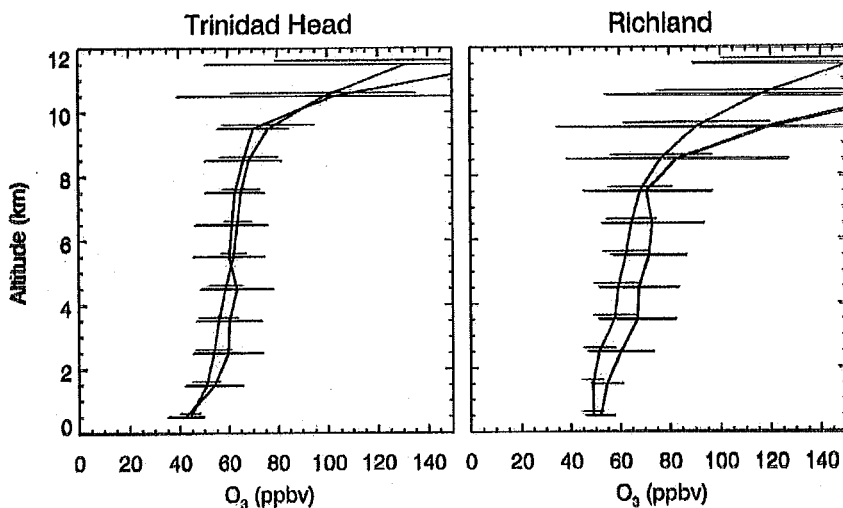


Fig. 5. Mean ozone concentration profiles over Trinidad Head, California ( $41^{\circ}$  N,  $124^{\circ}$  W) and Richland, Washington ( $46^{\circ}$  N,  $119^{\circ}$  W) during the INTEX-B campaign. The black lines show the means and standard deviations of ozonesonde data for the period of 17 April–15 May 2006 (13 sondes at Trinidad Head and 24 at Richland). The red lines show the corresponding means and standard deviations of model results with 2006 Asian emissions.

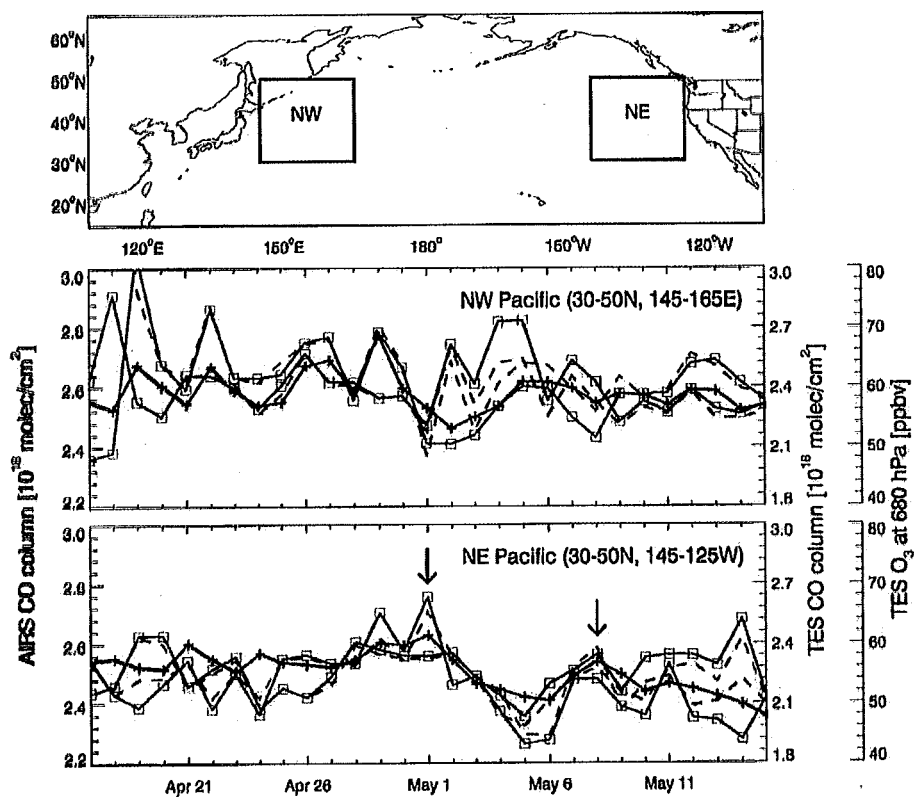
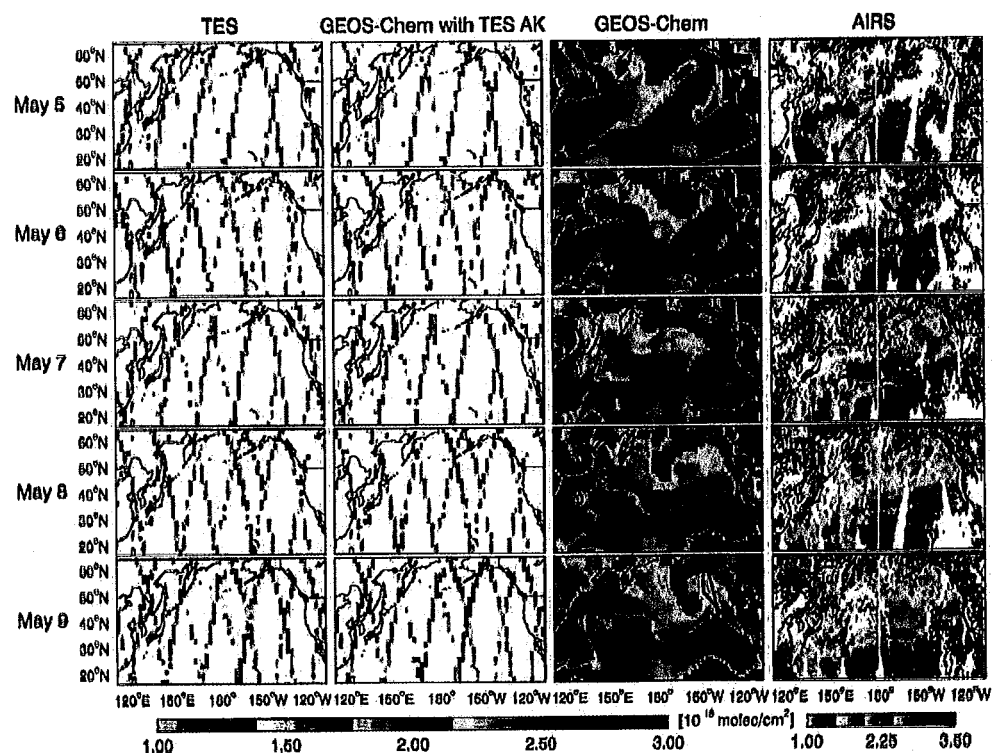


Fig. 6. Time series of AIRS and TES CO columns, and TES ozone at 680 hPa over the Northwest and Northeast Pacific during the INTEX-B time period. Two transpacific transport events are identified by arrows, reaching the Northeast Pacific on 1 and 8 May. The dashed lines show the time series of TES observations after filtering out stratospheric influence as described in the text.



**Fig. 7.** CO columns from AIRS, TES and the GEOS-Chem model during the 5–9 May transpacific Asian pollution event observed by the INTEX-B aircraft. GEOS-Chem values are sampled along the TES orbit tracks and with TES averaging kernels (AK) applied. The original TES data have been reprocessed to remove the effect of variable a priori and averaged on the model resolution. GEOS-Chem columns sampled at 12:00 UT without averaging kernels applied are also shown; the black line in the lower panel shows the INTEX-B DC-8 flight track on 9 May.

et al., 2003). CO shows a decreasing trend from April to May over the Northeast Pacific due to the seasonal decline of biomass burning in Southeast Asia (Duncan et al., 2003) and the seasonal increase of OH concentrations. The CO column data over the Northeast Pacific identify two major events of transpacific transport of Asian pollution during the INTEX-B period. The two events were also seen in situ observations. Event 1 was observed from the C-130 on 1 May (Bartlett et al., 2007), and was also observed at the MBO site as shown in Sect. 7.1. Event 2 was observed from the DC-8 on 9 May as discussed in Sect. 5.2, and arrived at MBO around 10 May.

TES observations of CO column show similar temporal variation as AIRS ( $r=0.75$  for both regions) but with larger variability. Figure 6 also shows TES observations of ozone concentrations retrieved at 680 hPa (corresponding to a broad mid-troposphere weighting function). The time series of TES CO and ozone observations are not always correlated. There are some periods with high ozone but low CO, such as 2 May over the Northwest Pacific and 14 May over the Northeast Pacific. Stratospheric intrusions occur ubiquitously throughout the midlatitudes (Cooper et al., 2004), and mixing Asian

pollution plumes with stratospheric air masses obscures the  $O_3$ -CO correlations (Nowak et al., 2004). After filtering out TES observations with stratospheric influence as diagnosed by TES  $O_3/CO$  at 680 hPa  $>0.6 \text{ mol mol}^{-1}$  (a stricter criterion than used for aircraft measurements due to the broad weighting functions in satellite retrievals), we find strong positive correlations ( $r>0.5$ , significant with 95% confidence) between the time series of TES CO and ozone observations for both regions. These correlations, likely driven by contrasts of Asian outflow and clean tropical marine air masses, suggest a combined export of ozone and CO pollution from the Asian continent. We examine this correlation in more detail below for a well-defined transpacific plume.

## 5.2 Transpacific transport event on 5–9 May

The transpacific event of 5–9 May was observed by both satellites and aircraft. Figure 7 shows daily AIRS and TES observations of CO for that period along with the corresponding GEOS-Chem simulation. AIRS with its high coverage illustrates the progression of the event and the GEOS-Chem

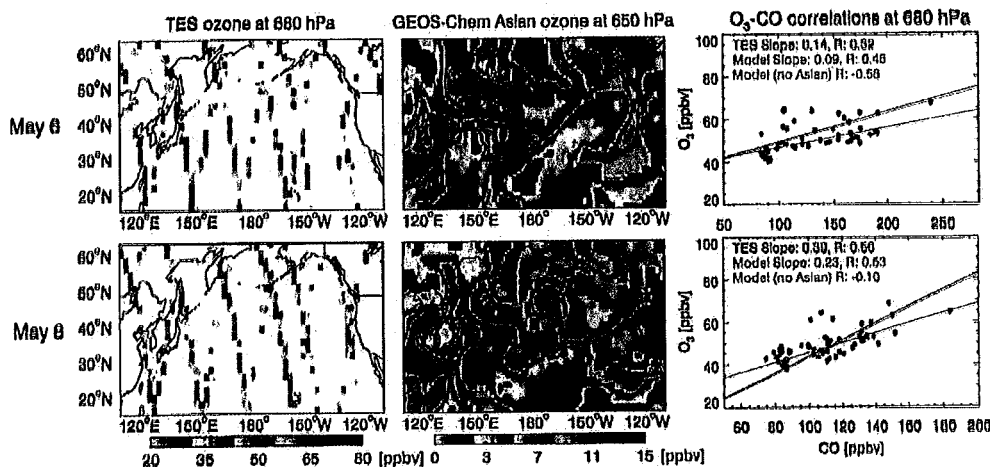


**Fig. 8.** (left) TES observations of ozone concentrations at 680 hPa on 6 and 8 May. The original TES data have been reprocessed to remove the effect of variable a priori and averaged on the  $2^{\circ} \times 2.5^{\circ}$  GEOS-Chem model grid. (center) Simulated Asian ozone enhancement on 6 and 8 May at 12:00 UTC, as determined by difference between the standard GEOS-Chem simulation and a simulation with Asian anthropogenic sources shut off. The black crosses show the locations of the TES observations of the Asian pollution plume used in the  $O_3$ -CO analysis. (right)  $O_3$ -CO relationships at 680 hPa for the plume shown in the central panel. The TES observations (black) are compared to model results from the standard simulation (red) and a sensitivity simulation with Asian emissions shut off (blue) sampled along the TES orbit tracks and with TES averaging kernels applied. Correlation coefficients ( $r$ ) and slopes of the reduced-major-axis regression lines ( $dO_3/dCO$ ,  $\text{mol mol}^{-1}$ ) are shown inset.

simulation is highly consistent. The Asian pollution plume is lifted with a southeastward moving front and rapidly transported in westerly winds at  $30^{\circ}$ – $50^{\circ}$  N across the Pacific. It splits into two air streams when crossing the Pacific high pressure system. The northern branch travels to Alaska in a circulation around the Aleutian Low, while the southern branch flows around the Pacific High and impacts the west coast of North America on 9 May.

Also shown in Fig. 7 are the GEOS-Chem model fields sampled along the TES orbit tracks and smoothed with TES averaging kernels. The model reproduces the variability observed by TES ( $r=0.80$ ). TES observations are relatively sparse but are qualitatively consistent with AIRS. Figure 8 shows the corresponding TES observations for ozone and the GEOS-Chem simulation of the Asian ozone pollution enhancement (determined by difference between the standard simulation and a sensitivity simulation with Asian anthropogenic sources shut off). Model results display a band of Asian ozone pollution accompanying CO and moving eastward within  $30^{\circ}$ – $50^{\circ}$  N, consistent with the pattern observed by TES.

Figure 8 (right panel) shows the correlations of TES ozone and CO measurements for the pollution plume at 680 hPa. Ozone and CO are positively correlated both in the TES observations and the model. The corresponding observed enhancement ratio  $dO_3/dCO=0.14 \pm 0.05 \text{ mol mol}^{-1}$  (standard deviation calculated by the bootstrap method, Venables and Ripley, 1999) on 6 May is smaller than summertime ob-

servations of  $0.2$ – $0.5 \text{ mol mol}^{-1}$  at surface sites in eastern North America (Parrish et al., 1993; Chin et al., 1994), and  $0.6 \text{ mol mol}^{-1}$  observed in Asian outflow by TES in July (Zhang et al., 2006). The smaller enhancement ratio is likely due to low photochemical activity in the springtime (Pierce et al., 2003). The larger  $dO_3/dCO$  ratio of  $0.39 \pm 0.12 \text{ mol mol}^{-1}$  observed on 8 May (with 90% confidence from t-test) is consistent with the typical ratios of  $0.2$ – $0.5 \text{ mol mol}^{-1}$  in industrial or biomass burning plumes from aircraft measurements over the Northeast Pacific in the spring (Price et al., 2004), and suggests continuous ozone production in the lower troposphere during transport across the Pacific. We see from Fig. 8 that the model reproduces the observed  $O_3$ -CO correlations at least qualitatively and these correlations disappear in a sensitivity simulation without Asian anthropogenic emissions, indicating that they are driven by Asian ozone pollution.

Figure 9 shows the aircraft vertical profiles sampling the pollution plume on the 9 May flight out of Anchorage (flight track shown in Fig. 7). The northern branch sampled at  $53^{\circ}$  N,  $150^{\circ}$  W, and 3.5–7 km altitude shows CO up to 182 ppbv and PAN up to 690 pptv. Ozone mixing ratios are about 65 ppbv, not significantly higher than the local background. The southern branch sampled at  $42^{\circ}$  N,  $138^{\circ}$  W, and 2.5–5.5 km altitude shows CO up to 206 ppbv and ozone up to 85 ppbv; PAN mixing ratios (125 pptv) are much lower than in the northern branch. The difference in ozone enhancements reflects the effect of subsidence

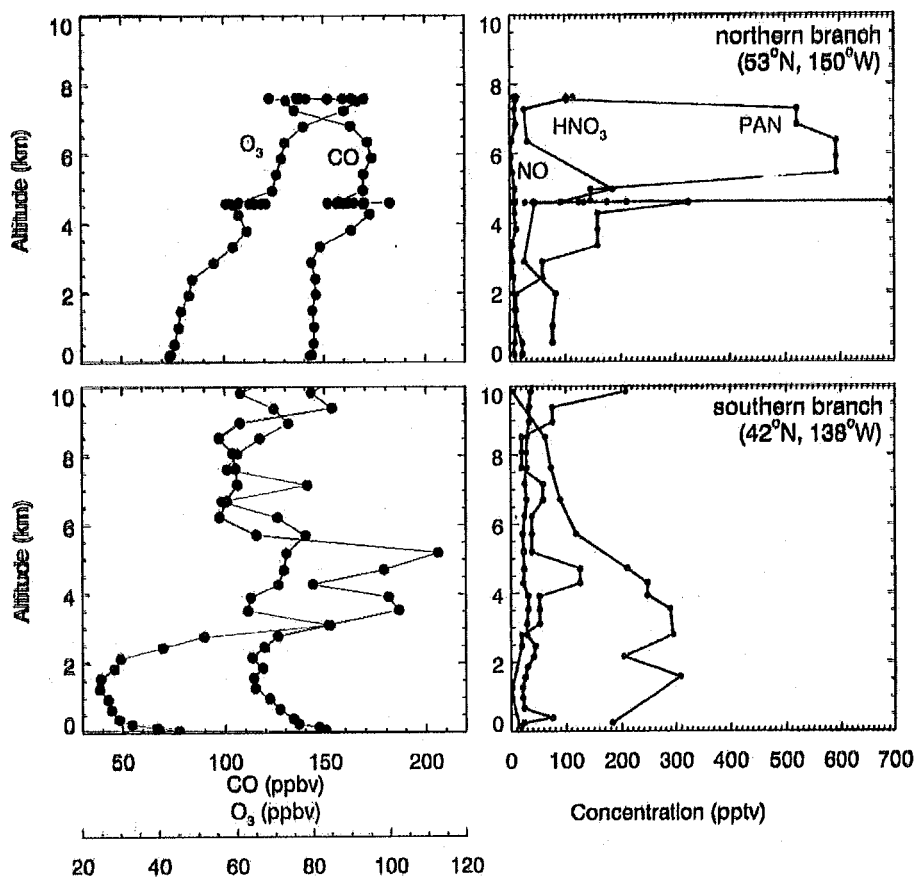


Fig. 9. Observed vertical profiles of concentrations for the northern (top) and southern (bottom) branches of the Asian pollution plume sampled by the INTEX-B DC-8 flight on 9 May. (left) CO (solid black) and ozone (solid red). (right)  $\text{NO}_y$  components: PAN (solid purple),  $\text{HNO}_3$  (solid blue), and NO (solid green).

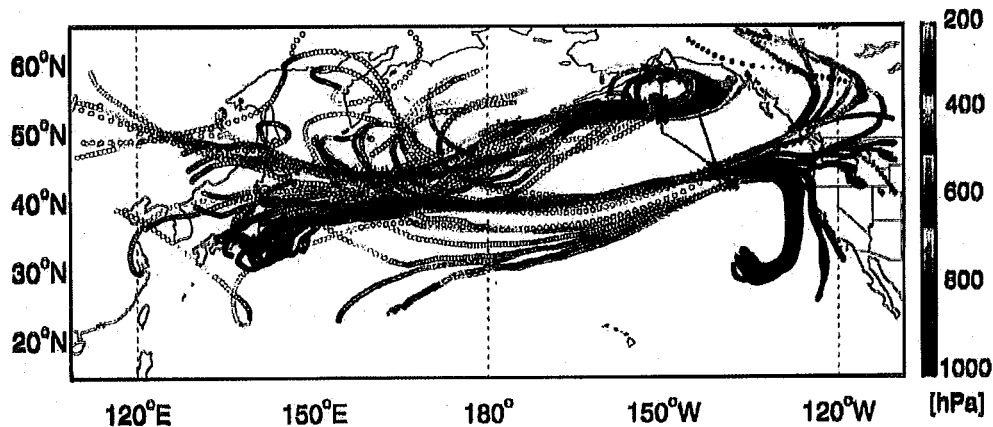
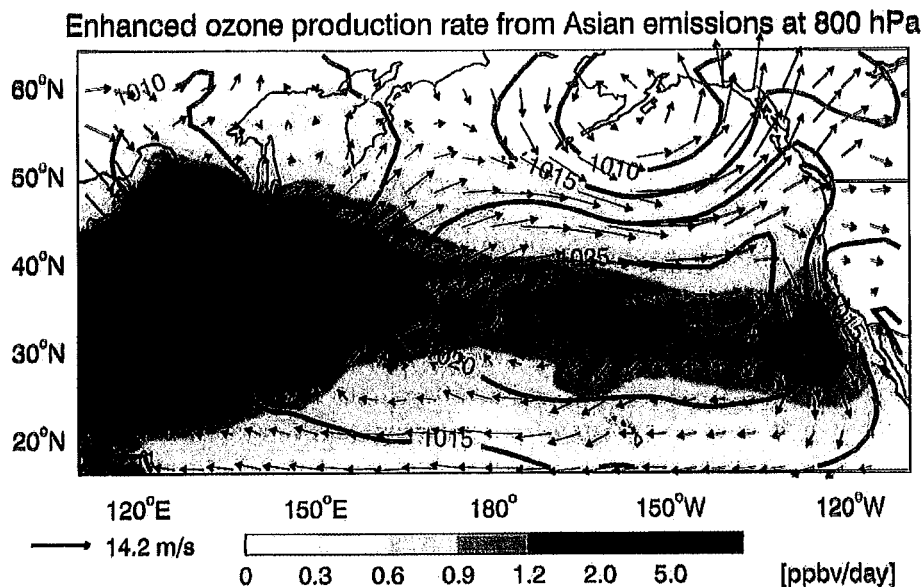
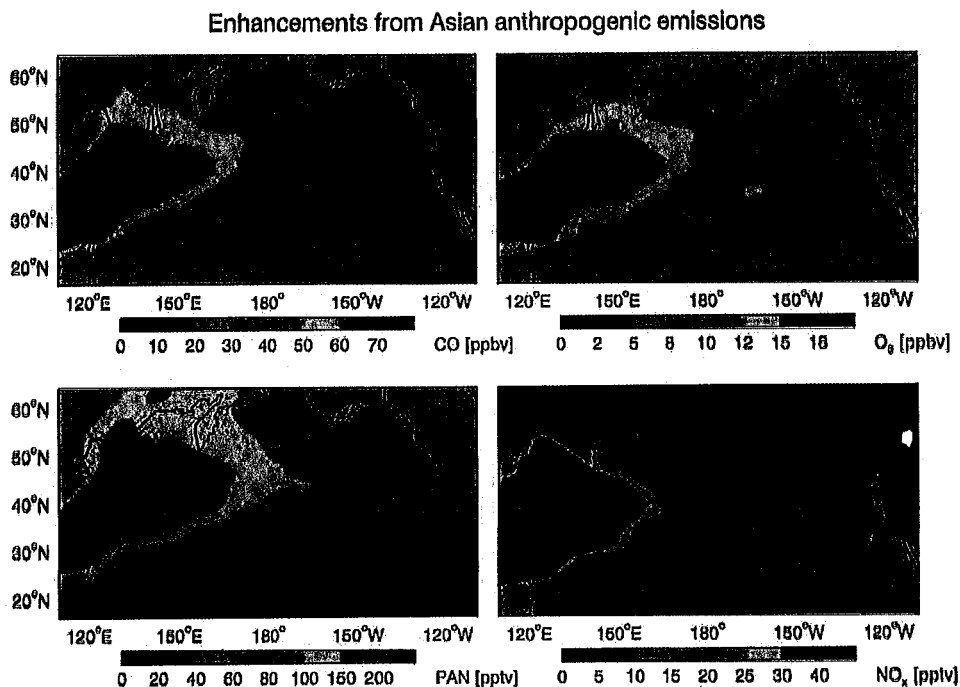


Fig. 10. Kinematic 7-day backward (open circles) and 3-day forward (solid circles) trajectories for the enhanced CO layers of Asian pollution ( $\text{CO} \geq 125$  ppbv and 2–7 km) observed in the INTEX-B DC-8 flight on May 9 as shown in Fig. 9. The flight track is shown in gray and the black crosses show the locations of enhanced CO layers, corresponding to the northern and southern branches of Fig. 9. The trajectories were constructed using reanalysis data from the National Centers for Environmental Prediction (Fuelberg et al., 2007).



**Fig. 11.** Mean gross ozone (odd oxygen) production rate at 800 hPa from anthropogenic Asian emissions during the INTEX-B period (17 April–15 May 2006). The Asian enhancement of ozone production is determined by the difference of gross ozone production rates between the standard simulation and a sensitivity simulation with Asian anthropogenic emissions shut off. The contours and vectors represent the mean GEOS-4 sea level pressures and 800 hPa wind fields for the period.



**Fig. 12.** Mean GEOS-Chem simulated Asian pollution enhancements of ozone, CO, NO<sub>x</sub>, and PAN at 800 hPa for the INTEX-B period (17 April–15 May 2006). The Asian pollution enhancements are determined by difference between the standard simulation and a sensitivity simulation with Asian anthropogenic emissions shut off.

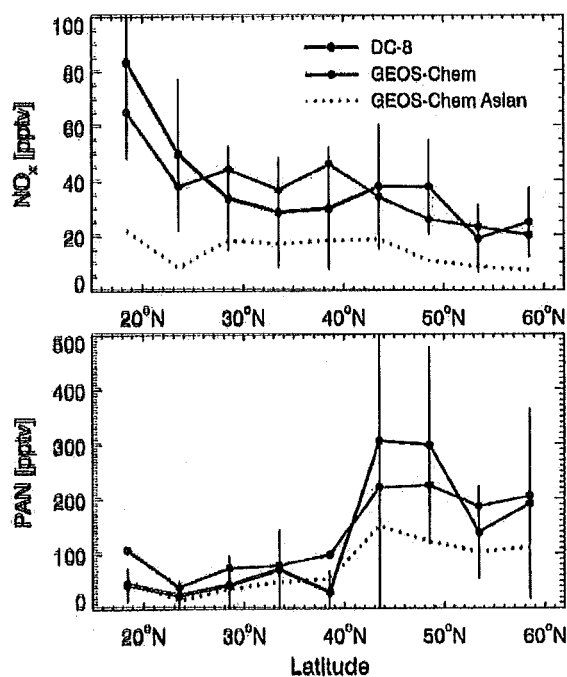


**Fig. 13.** Mean latitudinal distributions of  $\text{NO}_x$  and PAN concentrations over the Northeast Pacific at 1.5–5 km altitude during the INTEX-B period. Model results (red solid) are compared to the INTEX-B observations (black solid). Red dashed lines show the model Asian enhancements. Vertical bars are standard deviations of the observations.

driving PAN decomposition to  $\text{NO}_x$  and hence ozone production (Kotchenruther et al., 2001; Heald et al., 2003; Hess and Vukicevic, 2003; Hudman et al., 2004; Nowak et al., 2004).

The ozone production in the southern branch is relevant for direct impact on the United States. Figure 10 shows kinematic backward and forward trajectories based on reanalysis data from National Centers for Environmental Prediction (Fuelberg et al., 2007) for the enhanced CO layers of Asian pollution ( $\text{CO} > 125$  ppbv and 2–7 km) shown in Fig. 9. The 9 May flight measured distinct northern and southern branches of the plumes, but the backward trajectories in Fig. 10 demonstrate their common origin. The 3-day forward trajectories from the aircraft tracks show the different fates of the two pollution branches. The northern branch remains at high altitude over the Gulf of Alaska, while the southern branch subsides to impact the United States. However, a large part of that southern branch cycles around the Pacific High and avoids contact with North America.

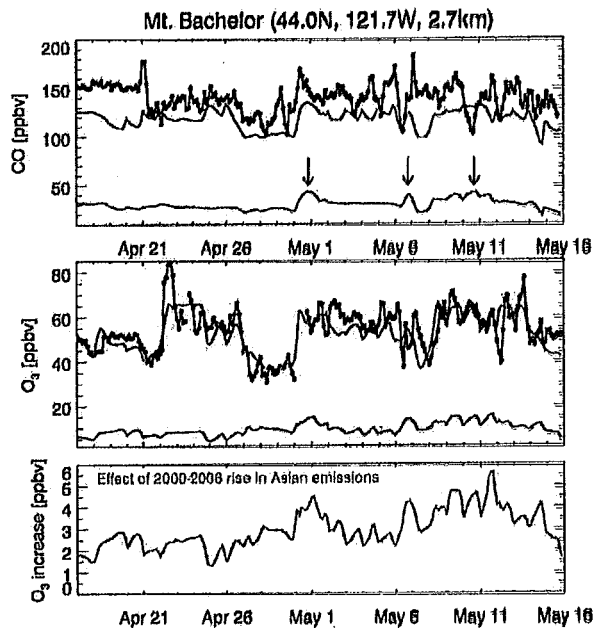


**Fig. 14.** Time series of 3-hourly averaged CO (top) and ozone (center) concentrations at MBO during the INTEX-B period. Model results (red) are compared to observations (black). The blue lines show the Asian anthropogenic enhancements in the model as determined by the difference between the standard simulation and a sensitivity simulation with Asian anthropogenic emissions shut off. Black arrows show Asian CO pollution maxima as indicated by the model. The bottom panel shows the simulated increase of ozone concentrations at MBO due to the rise of Asian anthropogenic emissions from 2000 to 2006.

## 6 Mean transpacific transport of Asian ozone and its precursors

We now generalize from the case study of 6–9 May to the mean transpacific Asian pollution influence during the INTEX-B period of 17 April–15 May, 2006. Figure 11 shows the mean enhancements of gross ozone production rates at 800 hPa due to Asian anthropogenic emissions, as determined by difference between the standard simulation and the sensitivity simulation with Asian anthropogenic emissions shut off. GEOS-Chem ozone production rates in the standard simulation are consistent with those from box models constrained by aircraft measurements over the Northwest Pacific (Auvray et al., 2007). Transpacific transport of ozone pollution mostly takes place in the free troposphere (Price et al., 2004), and we show 800 hPa in Fig. 11 as most relevant for North American air quality. We see fast production of Asian ozone pollution ( $> 5$  ppbv  $\text{d}^{-1}$ ) over the Asian continent where  $\text{NO}_x$  concentrations are high, but also sustained production ( $> 1$  ppbv  $\text{d}^{-1}$ ) across the Pacific at  $25^\circ\text{N}$ – $40^\circ\text{N}$  and a secondary maximum off the coast of California. Hudman et al. (2004) previously found that the ozone production

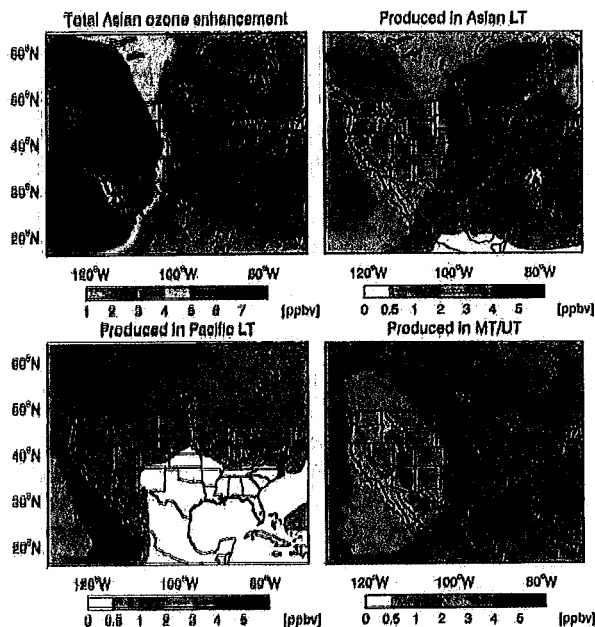


**Fig. 15.** Mean simulated US surface ozone enhancements from Asian anthropogenic emissions during the INTEX-B time period (17 April–15 May 2006). Total Asian ozone enhancements (top left) are separated into linear contributions from ozone produced in the Asian and Pacific lower troposphere (surface–700 hPa), and in the middle/upper troposphere (700 hPa–tropopause). Note that the top left panel has a different scale than the others.

efficiency is particularly high over the subsiding East Pacific because of the strong radiation and low humidity. This combined with the release of  $\text{NO}_x$  from PAN decomposition promotes relatively rapid ozone production ( $>1.5 \text{ ppbv d}^{-1}$ ).

Mean 800 hPa winds and sea level pressures for the INTEX-B period are also shown in Fig. 11. The Pacific High and Aleutian Low are prominent features and drive the westerly transport across the central and eastern Pacific (Liang et al., 2005). We see from Fig. 11 that splitting of Asian plumes over the Northeast Pacific is an expected feature of the mean circulation: the northern branch circulates around the Aleutian Low, while the southern branch circulates around the Pacific High and affects the western United States. As shown in Fig. 11, the high ozone production rate is limited to the southern branch. Most of the air in that southern branch actually skirts the US, as previously discussed in the May 5–9 case. It is instead entrained in the easterly tropical circulation to become the tropical “river of pollution” flowing back to the western equatorial Pacific in the marine boundary layer, as observed in the PEM-Tropics B aircraft campaign (Staudt et al., 2001; Martin et al., 2003).

Figure 12 shows the mean simulated Asian pollution enhancements of CO, PAN, ozone, and  $\text{NO}_x$  at 800 hPa for the INTEX-B period. They show the same pattern of Asian outflow but then become latitudinally separated during transport across the Pacific. CO and PAN have little production over the Pacific; their transport is mainly north of  $35^\circ \text{N}$ . By contrast, Asian ozone and  $\text{NO}_x$  are more enhanced at  $25^\circ \text{N}$ – $40^\circ \text{N}$ , corresponding to the southern branch of transpacific transport in Fig. 11 which provides a sustained source. The secondary maxima of Asian  $\text{NO}_x$  and ozone over the subtropical Pacific match the secondary maxima of Asian ozone production in Fig. 11.

The INTEX-B aircraft observations provide evidence for this latitudinal separation between Asian enrichments of  $\text{NO}_x$  and PAN. Figure 13 shows the mean observed and simulated latitudinal gradients of  $\text{NO}_x$  and PAN concentrations over the Northeast Pacific at 1.5–5 km altitude.  $\text{NO}_x$  concentrations decrease with increasing latitude while PAN increases with increasing latitude, with a step function at  $40^\circ \text{N}$ . The patterns are similar in the model and in the observations, confirming the mechanism of ozone production driven by PAN decomposition over the subtropical Pacific.

## 7 Impact of Asian pollution on North American surface ozone

### 7.1 Measurements at Mt. Bachelor Observatory

The Mt. Bachelor Observatory, a mountain site in central Oregon, is particularly sensitive to Asian influences due to its exposure to the free troposphere (Jaffe et al., 2005; Weiss-Penzias et al., 2006). We use measurements at MBO to test model estimates of Asian influence in North American background air. Figure 14 shows the 3-hourly observed and modeled time series of CO and ozone at MBO during the INTEX-B period. The model is unbiased for ozone and biased low by 20 ppbv for CO, as discussed previously in the context of the aircraft data. The synoptic-scale variability is well captured, particularly for ozone. The model predicts larger Asian pollution ozone enhancements in May than April due to increasing photochemical activity. May is climatologically the month of peak Asian influence on US ozone (Jacob et al., 1999). The day-to-day temporal variability of Asian ozone pollution simulated by the model is small, consistent with the previous analyses of Fiore et al. (2002) and Goldstein et al. (2004). Asian ozone pollution in the model mostly appears as a background enhancement rather than as discrete plumes. PAN concentrations measured at MBO during INTEX-B have a median of 270 pptv (Wolfe et al., 2007), compared to 190 pptv in GEOS-Chem, with fair agreement in temporal patterns between model and observations ( $r=0.56$ ).

Asian plumes with enhanced CO and ozone concentrations have been previously observed at MBO (Jaffe et al., 2005; Weiss-Penzias et al., 2007). The INTEX-B period is unusual

in that no strong plumes of CO were detected at MBO (Reidmiller et al., 2008). Arrows in Fig. 14 show Asian CO pollution maxima as indicated by the model and discussed further by Wolfe et al. (2007). Detecting these Asian pollution events in the CO observations is a challenge because of other, larger factors of variability. The observed CO enhancement on 1 May could be of Asian origin. The ozone observations show a coincident sharp increase but the model implies that only a small part of that increase is due to Asian emissions.

The mean observed ozone concentration at MBO during INTEX-B is  $54 \pm 10$  ppbv (mean  $\pm$  standard deviation), compared with  $53 \pm 9$  ppbv in the model. It is lower than the mean ozone observed at Trinidad Head and Richland at 2.7 km during INTEX-B (60 ppbv and 62 ppbv, respectively as shown in Fig. 5), because stratospheric influence at MBO is weaker (Weiss-Penzias et al., 2006). Asian anthropogenic emissions in the model increase ozone concentrations at MBO by  $9.2 \pm 2.5$  ppbv for the INTEX-B time period. Asian pollution is thus an important component of the model ozone background at MBO; without this contribution the model would greatly underestimate the measurements. In a previous study with the GEOS-Chem model, Hudman et al. (2004) found a mean Asian pollution enhancement of 7 ppbv ozone at a California mountain site in May 2002. The difference can be explained by rising Asian emissions. As shown in the bottom panel of Fig. 14, rising Asian emissions from 2000 to 2006 have increased ozone at MBO by 3 ppbv on average in April–May and up to 5 ppbv in events, although a small part of that increase could reflect the underestimate of emissions for Japan and Korea in the baseline S2000 inventory for 2000.

## 7.2 Impact on surface ozone air quality

Figure 15 (top left panel) shows the mean simulated surface ozone enhancement from Asian anthropogenic emissions over North America for the INTEX-B period. Asian ozone enhancements are 5–7 ppbv in the west and 2–5 ppbv in the east. The highest values are in the mountainous west.

To interpret these results we conducted two tagged  $O_x$  simulations, one using archived 3-D fields of daily production rates and loss frequencies from the standard simulation, and the other using those from the sensitivity simulation with Asian anthropogenic emissions shut off. The difference of the two simulations diagnoses the contributions from different production regions as sources of transpacific Asian ozone pollution. We thus distinguish in Fig. 15 between production in the Asian lower troposphere (up to 700 hPa), production in the Pacific lower troposphere (up to 700 hPa), and production in the middle and upper troposphere (above 700 hPa). Summation of these three tagged tracers gives the total Asian pollution ozone enhancement in the top left panel.

As shown in Fig. 15, most of the Asian ozone enhancement in western Canada is from transport of ozone produced in the Asian lower troposphere. The western United States and northern Mexico are more influenced by the south-

ern branch of transpacific transport, where continuous ozone production from exported Asian  $NO_x$  and PAN is comparable in magnitude to direct transport from the Asian boundary layer. Ozone production in the middle and upper troposphere is more important for US influence than in the subsiding air masses below 700 hPa (Pacific lower troposphere), as ozone produced in the latter region tends to remain over the subtropical Pacific rather than affect North America (Fig. 10 and 15).

Previous studies reported that pollution transported from Asia may contribute 3–5 ppbv to the ozone background over the western United States in the spring (Berntsen et al., 1999; Yienger et al., 2000). We find in the model that the 2000–2006 rise of Asian anthropogenic emissions increased surface ozone by 1–2 ppbv in the western United States (the larger impact of 3 ppbv at MBO is on account of its elevation). We conducted further sensitivity simulations to separate the contributions from the 100% rise in Asian  $NO_x$  emissions and the 45% rise in Asian NMVOC emissions, as the latter would affect PAN formation, and find that the ozone enhancement is most sensitive to  $NO_x$  emissions. The rise in Asian NMVOC emissions alone increases ozone by at most 0.4 ppbv anywhere in North America.

## 8 Conclusions

We used an ensemble of aircraft, satellite, sonde, and surface observations during the INTEX-B two-aircraft campaign over the Northeast Pacific (April–May 2006) to better understand and quantify the transpacific transport of Asian pollution and its effect on North American ozone air quality. We interpreted this ensemble of observations with a global 3-D model of tropospheric chemistry (GEOS-Chem). We addressed the impact of the recent rise in Asian emissions (2000–2006) on surface ozone air quality in North America.

Tropospheric  $NO_2$  column observations from the OMI satellite instrument provide top-down constraints on anthropogenic  $NO_x$  emissions in eastern Asia (including China, Japan, and Korea) in April–May 2006. We find a factor of 2 increase compared with the anthropogenic  $NO_x$  emission inventory from Streets et al. (2003) for the year 2000. This factor of 2 increase reflects a combination of 2000–2006 actual growth of Asian  $NO_x$  emissions (China) and an underestimate in the prior inventory (Korea, Japan). China accounted for over 80% of eastern Asian anthropogenic  $NO_x$  emissions as of 2006.

The model provides a good simulation of the ozone,  $NO_x$ , and PAN mean vertical profiles observed from the two INTEX-B aircraft. The simulation is only weakly sensitive to the 2000–2006 rise of Asian emissions in terms of comparison to observations; ozone increases by 3 ppbv on average. Simulated ozone over the west coast of North America is 5 ppb lower than observed from aircraft and ozonesondes during INTEX-B, which we attribute to

preferential stratospheric inflow over this region not resolved by the model. The model is 15% too low for CO compared to the aircraft observations, which we attribute tentatively to excessive OH (model values for OH are 27% higher than observed in INTEX-B).

Satellite observations of CO columns from AIRS and TES indicate at least two major events of transpacific Asian pollution during the INTEX-B time period. Tropospheric ozone observations from TES do not show a simple correlation with CO, reflecting at least in part the complicating effect of stratospheric influence. Filtering out this stratospheric influence reveals strong positive correlations between TES CO and ozone over the North Pacific. These correlations, likely driven by contrasts of Asian outflow and clean tropical marine air masses, indicate collocated export of ozone and CO pollution from the Asian continent.

We examined in detail a major transpacific Asian pollution plume sampled by the INTEX-B aircraft on 9 May. Measurements from AIRS and TES tracked the transpacific progression of this event. TES observed positive O<sub>3</sub>-CO correlations in the pollution plume, offering some evidence for net ozone production during transport across the Pacific. The plume split into northern and southern branches over the Northeast Pacific. Elevated ozone was observed by aircraft in the subsiding southern branch and was consistent with production from PAN decomposition.

Generalization to the mean transpacific Asian pollution influence during the INTEX-B period showed that this splitting of pollution plumes into two branches over the Northeast Pacific is an expected climatological feature driven by the circulations around the Pacific High and the Aleutian Low. The northern branch circulates around the Aleutian Low and remains at high altitude. The southern branch subsides around the Pacific High to affect the United States and northern Mexico, although most of that air skirts North America and is entrained in the easterly tropical circulation toward the western equatorial Pacific. Model results show high ozone production rates from Asian pollution in the southern branch, including a secondary maximum off the coast of California driven by subsidence. Concentrations of NO<sub>x</sub> and PAN measured from the aircraft show opposite latitudinal gradients in the lower troposphere, consistent with the model, and confirming the mechanism of PAN decomposition to NO<sub>x</sub> as a driver for transpacific ozone production.

We tested the model simulation of Asian pollution influences over North America with measurements at Mt. Bachelor Observatory (MBO) in central Oregon (2.7 km altitude). The model reproduces the ozone observations at MBO with no significant bias. Asian ozone pollution increases ozone concentrations in the model at MBO by  $9.2 \pm 2.5$  ppbv for the INTEX-B time period, representing an important contribution to total ozone in the model ( $53 \pm 9$  ppbv) and its ability to fit observations ( $54 \pm 10$  ppbv). The temporal variability of Asian ozone in the model is still small and undetectable in the observations. The 2000–2006 rise in Asian anthropogenic emissions increased model ozone at MBO by 3 ppbv on average and up to 5 ppbv in events.

We find that Asian anthropogenic emissions increased surface ozone concentrations by 5–7 ppbv in western North America during the INTEX-B period. The 2000–2006 rise in Asian anthropogenic emissions, including in particular the doubling of NO<sub>x</sub> emissions, increased that influence by 1–2 ppbv. Most of the Asian ozone pollution in western Canada originates from production in the lower troposphere over the Asian continent. The western United States and northern Mexico are more impacted by the southern branch of transpacific transport, which has sustained ozone production during transpacific transport driven by decomposition of PAN. About half of Asian anthropogenic ozone affecting the United States is produced in the Asian lower troposphere while the other half is produced during transpacific transport.

*Acknowledgements.* This work was funded by the NASA Global Tropospheric Chemistry Program and by NASA Headquarters under the Earth and Space Science Fellowship Program Grant NNX07AN65H to Lin Zhang.

Edited by: S. Madronich

## References

- Aumann, H. H., Chahine, M. T., Gautier, C., Goldberg, M. D., Kalnay, E., McMillin, L. M., Revercomb, H., Rosenkranz, P. W., Smith, W. L., Staelin, D. H., Strow, L. L., and Susskind, J.: AIRS/AMSU/HSB on the Aqua mission: Design, science objectives, data products and processing systems, *IEEE T. Geosci. Remote*, 41, 253–264, 2003.
- Auvray, M., Bey, I., Lhull, E., Schultz, M. G., and Rast, S.: A model investigation of tropospheric ozone chemical tendencies in long-range transported pollution plumes, *J. Geophys. Res.*, 112, D05304, doi:10.1029/2006JD007137, 2007.
- Barletta, B., Meinardi, S., Atlas, E., Blake, N. J., Baker, A. K., Beyersdorff, A. J., McKeachie, R., Midyett, J. R., Novak, B. J., Yang, M., and Blake, D. R.: Nonmethane Hydrocarbon (NMHC) Characterization of Asian Outflow During the INTEX-B Campaign: a Case Study from May 1, *Eos Trans. AGU*, 88(52), Fall Meet. Suppl., Abstract A33A-0822, 2007.
- Beer, R., Glavich, T. A., and Rider, D. M.: Tropospheric Emission Spectrometer for the Earth Observing System's Aura satellite, *Appl. Opt.*, 40, 2356–2367, 2001.
- Berntsen, T. K., Karlsdottir, S., and Jaffe, D. A.: Influence of Asian emissions on the composition of air reaching the Northwestern United States, *Geophys. Res. Lett.*, 26, 2171–2174, 1999.
- Bertschi, I. B., Jaffe, D. A., Jaeglé, L., Price, H. U., and Denison, J. B.: PHOBEA/ITCT 2002 airborne observations of trans-Pacific transport of ozone, CO, VOCs and aerosols to the northeast Pacific: Impacts of Asian anthropogenic and Siberian Boreal fire emissions, *J. Geophys. Res.*, 109, D23S12, doi:10.1029/2003JD004328, 2004.
- Bey, I., Jacob, D. J., Yantosca, R. M., Logan, J. A., Field, B. D., Fiore, A. M., Li, Q., Liu, H., Mickley, L. J., and Schultz, M. G.: Global modeling of tropospheric chemistry with assimilated me-

- teology: Model description and evaluation, *J. Geophys. Res.*, 106, 23 073–23 089, 2001.
- Boersma, K. F., Eskes, H. J., Veeckind, J. P., Brinkma, E. J., van der A, R. J., Sneep, M., van den Oord, G. H. J., Levelt, P. F., Stammes, P., Gleason, J. F., and Bucsela, E. J.: Near-real time retrieval of tropospheric NO<sub>2</sub> from OMI, *Atmos. Chem. Phys.*, 7, 2103–2118, 2007, <http://www.atmos-chem-phys.net/7/2103/2007/>.
- Boersma, K. F., Jacob, D. J., Bucsela, E. J., Perring, A. E., Dirksen, R., van der A, R. J., Yantosca, R. M., Park, R. J., Wenig, M. O., Bertram, T. H., and Cohen, R. C.: Validation of OMI tropospheric NO<sub>2</sub> observations during INTEX-B and application to constrain NO<sub>x</sub> emissions over the eastern United States and Mexico, *Atmos. Environ.*, 42(19), doi:10.1016/j.atmosenv.2008.02.004, 4480–4497, 2008.
- Bowman, K. W., Rodgers, C. D., Kulawik, S. S., Worden, J., Sarkissian, E., Osterman, G., Steck, T., Lou, M., Eldering, A., Shephard, M., Worden, H., Lampel, M., Clough, S., Brown, P., Rinsland, C., Gunson, M., and Beer, R.: Tropospheric emission spectrometer: Retrieval method and error analysis, *IEEE T. Geosci. Remote*, 44(5), 1297–1307, 2006.
- Brock, C. A., Hudson, P. K., Lovejoy, E. R., and et al.: Particle characteristics following cloud-modified transport from Asia to North America, *J. Geophys. Res.*, 109, D23S26, doi:10.1029/2003JD004198, 2004.
- Chen, G., Kleb, M. M., Brune, W. H., and Flocke, F. M.: An Overview of INTEX-B/MILAGRO/IMPEX Instrument and Measurement Intercomparison, *Eos Trans. AGU*, 88(52), Fall Meet. Suppl., Abstract A33A-0817, 2007.
- Chin, M., Jacob, D. J., Munger, J. W., Parrish, D. D., and Doddridge, B. G.: Relationship of ozone and carbon monoxide over North America, *J. Geophys. Res.*, 99, 14 565–14 573, 1994.
- Cooper, O. R., Forster, C., Parrish, D., Trainer, M., Dunlea, E., Ryerson, T., Hübler, G., Fehsenfeld, F., Nicks, D., Holloway, J., de Gouw, J., Warneke, C., Roberts, J. M., Flocke, F., and Moody, J.: A case study of transpacific warm conveyor belt transport: Influence of merging airstreams on trace gas import to North America, *J. Geophys. Res.*, 109, D23S08, doi:10.1029/2003JD003624, 2004.
- Dickerson, R. R., Li, C., Li, Z., Marufu, L. T., Stehr, J. W., McClure, B., Krotkov, N., Chen, H., Wang, P., Xia, X., Ban, X., Gong, F., Yuan, J., and Yang, J.: Aircraft observations of dust and pollutants over northeast China: Insight into the meteorological mechanisms of transport, *J. Geophys. Res.*, 112, D24S90, doi:10.1029/2007JD008999, 2007.
- Duncan, B. N., Martin, R. V., Staudt, A. C., Yevich, R., and Logan, J. A.: Interannual and seasonal variability of biomass burning emissions constrained by satellite observations, *J. Geophys. Res.*, 108(D2), 4100, doi:10.1029/2002JD002378, 2003.
- Fiore, A. M., Jacob, D. J., Bey, I., Yantosca, R. M., Field, B. D., Fusco, A. C., and Wilkinson, J. G.: Background ozone over the United States in summer: Origin, trend, and contribution to pollution episodes, *J. Geophys. Res.*, 107(D15), 4275, doi:10.1029/2001JD000982, 2002.
- Fiore, A., Jacob, D. J., Liu, H., Yantosca, R. M., Fairlie, T. D., and Li, Q.: Variability in surface ozone background over the United States: Implications for air quality policy, *J. Geophys. Res.*, 108(D24), 4787, doi:10.1029/2003JD003855, 2003.
- Forster, C., Cooper, O., Stohl, A., Eckhardt, S., James, P., Dunlea, E., Nicks Jr., D. K., Holloway, J. S., Hübler, G., Parrish, D. D., Ryerson, T. B., and Trainer, M.: Lagrangian transport model forecasts and a transport climatology for the Intercontinental Transport and Chemical Transformation 2002 (ITCT 2K2) measurement campaign, *J. Geophys. Res.*, 109, D07S92, doi:10.1029/2003JD003589, 2004.
- Fuelberg, H. E., Porter, M. J., Kiley, C. M., Halland, J. J., and Morse, D.: Meteorological conditions and anomalies during the Intercontinental Chemical Transport Experiment–North America, *J. Geophys. Res.*, 112, D12S06, doi:10.1029/2006JD007734, 2007.
- Goldstein, A. H., Millet, D. B., McKay, M., Jaeglé, L., Horowitz, L., Cooper, O., Hudman, R., Jacob, D. J., Oltmans, S., and Clarke, A.: Impact of Asian emissions on observations at Trinidad Head, California, during ITCT 2K2, *J. Geophys. Res.*, 109, D23S17, doi:10.1029/2003JD004406, 2004.
- Heald, C. L., Jacob, D. J., Fiore, A. M., Emmons, L. K., Gille, J. C., Deeter, M. N., Warner, J., Edwards, D. P., Crawford, J. H., Hamilton, A. J., Sachse, G. W., Browell, E. V., Avery, M. A., Vay, S. A., Westberg, D. J., Blake, D. R., Singh, H. B., Sandholm, S. T., Talbot, R. W., and Fuelberg, H. E.: Asian outflow and transpacific transport of carbon monoxide and ozone pollution: An integrated satellite, aircraft and model perspective, *J. Geophys. Res.*, 108(D24), 4804, doi:10.1029/2003JD003507, 2003.
- Heald, C. L., Jacob, D. J., Park, R. J., Alexander, B., Fairlie, D., Yantosca, R. M., and Chu, A.: Transpacific transport of Asian anthropogenic aerosols and its impact on surface air quality in the United States, *J. Geophys. Res.*, 111, D14310, doi:10.1029/2005JD006847, 2006.
- Hess, P. G. and Vukicevic, T.: Intercontinental transport, chemical transformations, and baroclinic systems, *J. Geophys. Res.*, 108(D12), 4354, doi:10.1029/2002JD002798, 2003.
- Hudman, R. C., Jacob, D. J., Cooper, O. R., Evans, M. J., Heald, C. L., Park, R. J., Fehsenfeld, F., Flocke, F., Holloway, J., Hübler, G., Kita, K., Koike, M., Kondo, Y., Neuman, A., Nowak, J., Oltmans, S., Parrish, D., Roberts, J. M., and Ryerson, T.: Ozone production in transpacific Asian pollution plumes and implications for ozone air quality in California, *J. Geophys. Res.*, 109, D23S10, doi:10.1029/2004JD004974, 2004.
- Hudman, R. C., Jacob, D. J., Turquety, S., Leibensperger, E. M., Murray, L. T., Wu, S., Gilliland, A. B., Avery, M., Bertram, T. H., Brune, W., Cohen, R. C., Dibb, J. E., Flocke, F. M., Fried, A., Holloway, J., Neuman, J. A., Orville, R., Perring, A., Ren, X., Sachse, G. W., Singh, H. B., Swanson, A., and Woodriddle, P. J.: Surface and lightning sources of nitrogen oxides over the United States: Magnitudes, chemical evolution, and outflow, *J. Geophys. Res.*, 112, D12S05, doi:10.1029/2006JD007912, 2007.
- Huntrieser, H., Schlager, H., Höller, H., Schumann, U., Betz, H. D., Boccippio, D., Brunner, D., Forster, C., and Stohl, A.: Lightning produced NO<sub>x</sub> in tropical, subtropical and midlatitude thunderstorms: New insights from airborne and lightning observations, *Geophys. Res. Abstr.*, 8, 03286, SRef-ID:1607-7962/gra/BGU06-A-03286, 2006.
- Jaeglé, L., Jaffe, D. A., Price, H. U., Weiss, P., Palmer, P. I., Evans, M. J., Jacob, D. J., and Bey, I.: Sources and budgets for CO and O<sub>3</sub> in the Northeastern Pacific during the spring of 2001: Results from the PHOBEA-II Experiment, *J. Geophys. Res.*, 108(D20), 8802, doi:10.1029/2002JD003121, 2003.
- Jaeglé, L., Steinberger, L., Martin, R. V., and Chance, K.: Global

- partitioning of  $\text{NO}_x$  sources using satellite observations: Relative roles of fossil fuel combustion, biomass burning and soil emissions, *Faraday Disc.*, 130, 407–423, 2005.
- Jacob, D. J., Logan, J. A., Gardner, G. M., Yevich, R. M., Spivakovsky, C. M., Wofsy, S. C., Sillman, S., and Prather, M. J.: Factors regulating ozone over the United States and its export to the global atmosphere, *J. Geophys. Res.*, 98, 14 817–14 826, 1993.
- Jacob, D. J., Heikes, B. G., Fan, S.-M., Logan, J. A., Mauzerall, D. L., Bradshaw, J. D., Singh, H. B., Gregory, G. L., Talbot, R. W., Blake, D. R., and Sachse, G. W.: Origin of ozone and  $\text{NO}_x$  in the tropical troposphere: A photochemical analysis of aircraft observations over the South Atlantic basin, *J. Geophys. Res.*, 101, 24 235–24 250, 1996.
- Jacob, D. J., Logan, J. A., and Murti, P. P.: Effect of rising emissions on surface ozone in the United States, *Geophys. Res. Lett.*, 26, 2175–2178, 1999.
- Jaffe, D. A., Anderson, T., Covert, D., Trost, B., Danielson, J., Simpson, W., Blake, D., Harris, J., and Streets, D.: Observations of ozone and related species in the northeast Pacific during the PHOBEA campaigns: 1. Ground-based observations as Cheeka Peak, *J. Geophys. Res.*, 106, 7449–7461, 2001.
- Jaffe, D., Price, H., Parrish, D. D., Goldstein, A., and Harris, J.: Increasing background ozone during spring on the west coast of North America, *Geophys. Res. Lett.*, 30(12), 1613, doi:10.1029/2003GL017024, 2003.
- Jaffe, D., Prestbo, E., Swartzendruber, P., Weiss-Penzias, P., Kato, S., Takami, A., Hatakeyama, S., and Kajii, Y.: Export of atmospheric mercury from Asia, *Atmos. Environ.*, 39, 3029–3038, 2005.
- Jaffe, D. A. and Ray, J.: Increase in surface ozone at rural sites in the western US, *Atmos. Environ.*, 41, 5452–5463, 2007.
- Jaffe, D. A., Thornton, J., Wolfe, G., Reidmiller, D., Fischer, E. V., Jacob, D. J., Zhang, L., Cohen, R., Singh, H., Weinheimer, A., and Flocke, F.: Can we detect an influence over North America from increasing Asian  $\text{NO}_x$  emissions?, *Eos Trans. AGU*, 88(52), Fall Meet. Suppl., Abstract A51E-04, 2007.
- Kiley, C. M. and Fuelberg, H. E.: An examination of summertime cyclone transport processes during Intercontinental Chemical Transport Experiment (INTEX-A), *J. Geophys. Res.*, 111, D24S06, doi:10.1029/2006JD007115, 2006.
- Kotchenruther, R. A., Jaffe, D. A., and Jaeglé, L.: Ozone Photochemistry and the Role of PAN in the Springtime Northeastern Pacific Troposphere: Results from the PHOBEA Campaign, *J. Geophys. Res.*, 106, 28 731–28 741, 2001.
- Latto, A. and Fuelberg, H.: Quasi-Lagrangian Chemical Sampling during INTEX-B, *Eos Trans. AGU*, 88(52), Fall Meet. Suppl., Abstract A42A-08, 2007.
- Levelt, P. F., van den Oord, G. H. J., Dobber, M. R., Mälkki, A., Visser, H., de Vries, J., Stammes, P., Lundell, J. O. V., and Saari, H.: The Ozone Monitoring Instrument, *IEEE T. Geosci. Remote*, 44(5), 1093–1101, 2006.
- Li, Q., Jacob, D. J., Bey, I., Palmer, P. I., Duncan, B. N., Field, B. D., Martin, R. V., Fiore, A. M., Yantosca, R. M., Parrish, D. D., Simmonds, P. G., and Oltmans, S. J.: Transatlantic transport of pollution and its effects on surface ozone in Europe and North America, *J. Geophys. Res.*, 107(D13), 4166, doi:10.1029/2001JD001422, 2002.
- Liang, Q., Jaeglé, L., Jaffe, D. A., Weiss-Penzias, P., Heckman, A., and Snow, J. A.: Long-range transport of Asian pollution to the northeast Pacific: Seasonal variations and transport pathways of carbon monoxide, *J. Geophys. Res.*, 109, D23S07, doi:10.1029/2003JD004402, 2004.
- Liang, Q., Jaeglé, L., and Wallace, J. M.: Meteorological indices for Asian outflow and transpacific transport on daily to interannual timescales, *J. Geophys. Res.*, 110, D18308, doi:10.1029/2005JD005788, 2005.
- Liang, Q., Jaeglé, L., Hudman, R. C., Turquety, S., Jacob, D. J., Avery, M. A., Browell, E. V., Sachse, G. W., Blake, D. R., Brune, W., Ren, X., Cohen, R. C., Dibb, J. E., Fried, A., Fuelberg, H., Porter, M., Heikes, B. G., Huey, G., Singh, H. B., and Wennberg, P. O.: Summertime influence of Asian pollution in the free troposphere over North America, *J. Geophys. Res.*, 112, D12S11, doi:10.1029/2006JD007919, 2007.
- Liu, S. C., Trainer, M., Fehsenfeld, F. C., Parrish, D. D., Williams, E. J., Fahey, D. W., Gubler, G., and Murphy, P. C.: Ozone production in the rural troposphere and the implications for regional and global ozone distributions, *J. Geophys. Res.*, 92, 4191–4207, 1987.
- Liu, H., Jacob, D. J., Bey, I., Yantosca, R. M., Duncan, B. N., and Sachse, G. W.: Transport pathways for Asian pollution outflow over the Pacific: Interannual and seasonal variations, *J. Geophys. Res.*, 108(D20), 8786, doi:10.1029/2002JD003102, 2003.
- Liu, J. and Mauzerall, D. L.: Estimating the average time for intercontinental transport of air pollutants, *Geophys. Res. Lett.*, 32, L11814, doi:10.1029/2005GL022619, 2005.
- Luo, M., Rinsland, C. P., Rodgers, C. D., Logan, J. A., Worden, H., Kulawik, S., Eldering, A., Goldman, A., Shephard, M. W., Guntson, M., and Lampel, M.: Carbon monoxide measurements by TES and MOPITT – the influence of a priori data and instrument characteristics on nadir atmospheric species retrievals, *J. Geophys. Res.*, 112, D09303, doi:10.1029/2006JD007663, 2007a.
- Luo, M., Rinsland, C., Fisher, B., Sachse, G., Diskin, G., Logan, J., Worden, H., Kulawik, S., Osterman, G., Eldering, A., Herman, R., and Shephard, M.: TES carbon monoxide validation with DACOM aircraft measurements during INTEX-B 2006, *J. Geophys. Res.*, 112, D24S48, doi:10.1029/2007JD008803, 2007b.
- Martin, B. D., Fuelberg, H. E., Blake, N. J., Crawford, J. H., Logan, J. A., Blake, D. R., and Sachse, G. W.: Long range transport of Asian outflow to the equatorial Pacific, *J. Geophys. Res.*, 108(D2), 8322, doi:10.1029/2001JD001418, 2003.
- Martin, R. V., Jacob, D. J., Chance, K., Kurosu, T. P., Palmer, P. I., and Evans, M. J.: Global inventory of nitrogen oxide emissions constrained by space-based observations of  $\text{NO}_2$  columns, *J. Geophys. Res.*, 108(D17), 4537, doi:10.1029/2003JD003453, 2003.
- Martin, R. V., Sioris, C. E., Chance, K., Ryerson, T. B., Bertram, T. H., Wooldridge, P. J., Cohen, R. C., Neuman, J. A., Swanson, A., and Flocke, F. M.: Evaluation of space-based constraints on global nitrogen oxide emissions with regional aircraft measurements over and downwind of eastern North America, *J. Geophys. Res.*, 111, D15308, doi:10.1029/2005JD006680, 2006.
- McLinden, C. A., Olsen, S. C., Hannegan, B., Wild, O., Prather, M. J., and Sundet, J.: Stratospheric ozone in 3-D models: A simple chemistry and the cross-tropopause flux, *J. Geophys. Res.*, 105(D11), 14 653–14 666, 2000.
- McMillan, W. W., Barnet, C., Strow, L., Chahine, M., Warner, J., McCourt, M., Novelli, P., Korontzi, S., Maddy, E., and Datta,

- S.: Daily global maps of carbon monoxide from NASA's Atmospheric Infrared Sounder, *Geophys. Res. Lett.*, 32, L11801, doi:10.1029/2004GL021821, 2005.
- McMillan, W. W., Warner, J. X., Comer, M. M., et al.: AIRS views of transport from 12–22 July 2004 Alaskan/Canadian fires: Correlation of AIRS CO and MODIS AOD with forward trajectories and comparison of AIRS CO retrievals with DC-8 in situ measurements during INTEX-A/ICARTT, *J. Geophys. Res.*, in review, 2008.
- Nassar, R., Logan, J. A., Worden, H. M., et al.: Validation of tropospheric emissions spectrometer (TES) nadir ozone profiles using ozonesonde measurements, *J. Geophys. Res.*, 113, in press, doi:10.1029/2007JD008819, 2008.
- Nowak, J. B., Parrish, D. D., Neuman, J. A., Holloway, J. S., Cooper, O. R., Ryerson, T. B., Nicks Jr., D. K., Flocke, F., Roberts, J. M., Atlas, E., de Gouw, J. A., Donnelly, S., Dunlea, E., Hübler, G., Huey, L. G., Schauffler, S., Tanner, D. J., Warnecke, C., and Fehsenfeld, F. C.: Gas-phase chemical characteristics of Asian emission plumes observed during ITCT 2K2 over the eastern North Pacific Ocean, *J. Geophys. Res.*, 109, D23S19, doi:10.1029/2003JD004488, 2004.
- Ohara, T., Akimoto, H., Kurokawa, J., Horii, N., Yamaji, K., Yan, X., and Hayasaka, T.: An Asian emission inventory of anthropogenic emission sources for the period 1980–2020, *Atmos. Chem. Phys.*, 7, 4419–4444, 2007, <http://www.atmos-chem-phys.net/7/4419/2007/>.
- Olson, J. R., Crawford, J. H., Chen, G., Brune, W. H., Faloon, I. C., Tan, D., Harder, H., and Martinez, M.: A reevaluation of airborne HO<sub>x</sub> observations from NASA field campaigns, *J. Geophys. Res.*, 111, D10301, doi:10.1029/2005JD006617, 2006.
- Park, R. J., Jacob, D. J., Field, B. D., Yantosca, R. M., and Chin, M.: Natural and trans-boundary pollution influences on sulfate-nitrate-ammonium aerosols in the United States: Implications for policy, *J. Geophys. Res.*, 109, D15204, doi:10.1029/2003JD004473, 2004.
- Parrish, D. D., Holloway, J. S., Trainer, M., Murphy, P. C., Fehsenfeld, F. C., and Forbes, G. L.: Export of North America ozone pollution to the North Atlantic Ocean, *Science*, 259, 1436–1439, 1993.
- Pierce, R. B., Al-Saadi, J. A., Schaack, T., Lenzen, A., Zapotocny, T., Johnson, D., Kittaka, C., Buker, M., Hitchman, M. H., Tripoli, G., Fairlie, T. D., Olson, J. R., Natarajan, M., Crawford, J., Fishman, J., Avery, M., Browell, E. V., Creilson, J., Kondo, Y., and Sandholm, S. T.: Regional Air Quality Modeling System (RAQMS) predictions of the tropospheric ozone budget over east Asia, *J. Geophys. Res.*, 108(D21), 8825, doi:10.1029/2002JD003176, 2003.
- Pickering, K. E., Wang, Y. S., Tao, W. K., Price, C., and Muller, J. F.: Vertical distributions of lightning NO<sub>x</sub> for use in regional and global chemical transport models, *J. Geophys. Res.*, 103, 31 203–31 216, 1998.
- Prather, M. J. and Ehhalt, D.: Chapter 4: Atmospheric Chemistry and Greenhouse Gases, in *Climate Change 2001: The Science of Climate Change*, Intergovernmental Panel on Climate Change, Cambridge University Press, 260–263, 2001.
- Price, C. and Rind, D.: A simple lightning parameterization for calculating global lightning distributions, *J. Geophys. Res.*, 97, 9919–9933, 1992.
- Price, H. U., Jaffe, D. A., Cooper, O. R., and Doskey, P. V.: Photochemistry, ozone production, and dilution during long-range transport episodes from Eurasia to the northwest United States, *J. Geophys. Res.*, 109, D23S13, doi:10.1029/2003JD004400, 2004.
- Reidmiller, D. R., Jaffe, D. A., Chand, D., Strode, S., Swartzendruber, P., Wolfe, G. M., and Thornton, J. A.: Interannual variability of long-range transport as seen at the Mt. Bachelor Observatory, *Atmos. Chem. Phys. Discuss.*, 8, 16 335–16 379, 2008, <http://www.atmos-chem-phys-discuss.net/8/16335/2008/>.
- Ren, X., Mao, J., Chen, Z., Brune, W., Olson, J., Crawford, J., Chen, G.: HO<sub>x</sub> Chemistry and Ozone Production During INTEX-B, *Eos Trans. AGU*, 88(52), Fall Meet. Suppl., Abstract A42A-04, 2007.
- Richards, N. A. D., Osterman, G. B., Browell, E. V., Hair, J. W., Avery M., and Li, Q.: Validation of Tropospheric Emission Spectrometer (TES) Ozone Profiles with Aircraft Observations During INTEX-B, *J. Geophys. Res.*, 113, D16S29, doi:10.1029/2007JD008815, 2008.
- Richter, A., Burrows, J. P., Nüß, H., Granier, C., and Niemeier, U.: Increase in tropospheric nitrogen dioxide levels over China observed from space, *Nature*, 437, 129–132, 2005.
- Staudt, A. C., Jacob, D. J., Logan, J. A., Bachiochi, D., Krishnamurti, T. N., and Sachse, G. W.: Continental sources, transoceanic transport, and interhemispheric exchange of carbon monoxide over the Pacific, *J. Geophys. Res.*, 106, 32 571–32 590, 2001.
- Stohl, A., Eckhardt, S., Forster, C., James, P., and Spichtinger, N.: On the pathways and timescales of intercontinental air pollution transport, *J. Geophys. Res.*, 107(D23), 4684, doi:10.1029/2001JD001396, 2002.
- Streets, D. G., Bond, T. C., Carmichael, G. R., Fernandes, S. D., Fu, Q., He, D., Klimont, Z., Nelson, S. M., Tsai, N. Y., Wang, M. Q., Woo, J.-H., and Yarber, K. F.: An inventory of gaseous and primary aerosol emissions in Asia in the year 2000, *J. Geophys. Res.*, 108(D21), 8809, doi:10.1029/2002JD003093, 2003.
- Streets, D. G., Zhang, Q., Wang, L., He, K., Hao, J., Wu, Y., Tang, Y., and Carmichael, G. R.: Revisiting China's CO emissions after TRACE-P: Synthesis of inventories, atmospheric modeling, and observations, *J. Geophys. Res.*, 111, D14306, doi:10.1029/2006JD007118, 2006.
- Sudo, K. and Akimoto, H.: Global source attribution of tropospheric ozone: Long-range transport from various source regions, *J. Geophys. Res.*, 112, D12302, doi:10.1029/2006JD007992, 2007.
- Thompson, A. M., Pickering, K. E., Dickerson, R. R., Ellis, W. G., Jacob, D. J., Scala, J. R., Tao, W. K., McNamara, D. P., and Simpson, J.: Convective transport over the central United States and its role in regional CO and ozone budgets, *J. Geophys. Res.*, 99(D9), 18 703–18 711, 1994.
- Thompson, A. M., Pickering, K. E., McNamara, D. P., Schoeberl, M. R., Hudson, R. D., Kim, J.-H., Browell, E. V., Kirchhoff, V. W. J. H., and Nganga, D.: Where did tropospheric ozone over southern Africa and the tropical Atlantic come from in October 1992? Insights from TOMS, GTE/TRACE-A and SAFARI-92, *J. Geophys. Res.*, 101, 24 251–24 278, 1996.
- Thompson, A. M., Yorks, J. E., Miller, S. K., Witte, J. C., Dougherty, K. M., Morris, G. A., Baumgardner, D., Ladino, L., and Rappenglück, B.: Tropospheric ozone sources and wave activity over Mexico City and Houston during

- MILAGRO/Intercontinental Transport Experiment (INTEX-B) Ozone-sonde Network Study, 2006 (IONS-06), *Atmos. Chem. Phys.*, 8, 5113–5125, 2008, <http://www.atmos-chem-phys.net/8/5113/2008/>.
- van der A, R. J., Peters, D. H. M. U., Eskes, H., Boersma, K. F., Van Roozendaal, M., De Smedt, I., and Kelder, H. M.: Detection of the trend and seasonal variation in tropospheric NO<sub>2</sub> over China, *J. Geophys. Res.*, 111, D12317, doi:10.1029/2005JD006594, 2006.
- van der Werf, G. R., Randerson, J. T., Giglio, L., Collatz, G. J., Kasibhatla, P. S., and Arellano Jr., A. F.: Interannual variability in global biomass burning emissions from 1997 to 2004, *Atmos. Chem. Phys.*, 6, 3423–3441, 2006, <http://www.atmos-chem-phys.net/6/3423/2006/>.
- Venables, W. N. and Ripley, B. D.: *Modern Applied Statistics with S-PLUS*, 3rd ed., Springer-Verlag, New York, p. 501, 1999.
- Wang, Y., Jacob, D. J., and Logan, J. A.: Global simulation of tropospheric O<sub>3</sub>-NO<sub>x</sub>-hydrocarbon chemistry 1. Model formulation, *J. Geophys. Res.*, 103(D9), 10 713–10 726, 1998a.
- Wang, Y., Jacob, D. J., and Logan, J. A.: Global simulation of tropospheric O<sub>3</sub>-NO<sub>x</sub>-hydrocarbon chemistry, 3. Origin of tropospheric ozone and effects of non-methane hydrocarbons, *J. Geophys. Res.*, 103/D9, 10 757–10 768, 1998b.
- Wang, Y. X., McElroy, M. B., Martin, R. V., Streets, D. G., Zhang, Q., and Fu, T.-M.: Seasonal variability of NO<sub>x</sub> emissions over east China constrained by satellite observations: Implications for combustion and microbial sources, *J. Geophys. Res.*, 112, D06301, doi:10.1029/2006JD007538, 2007.
- Warner, J., Comer, M. M., Barnet, C. D., McMillan, W. W., Wolf, W., Maddy, E., and Sachse, G.: A comparison of satellite tropospheric carbon monoxide measurements from AIRS and MOPITT during INTEX-A, *J. Geophys. Res.*, 112, D12S17, doi:10.1029/2006JD007925, 2007.
- Weiss-Penzias, P., Jaffe, D. A., Jaeglé, L., and Liang, Q.: Influence of long-range-transported pollution on the annual and diurnal cycles of carbon monoxide and ozone at Cheeka Peak Observatory, *J. Geophys. Res.*, 109, D23S14, doi:10.1029/2004JD004505, 2004.
- Weiss-Penzias, P., Jaffe, D. A., Swartzendruber, P., Dennison, J. B., Chand, D., Hafner, W., and Prestbo, E.: Observations of Asian air pollution in the free troposphere at Mount Bachelor Observatory during the spring of 2004, *J. Geophys. Res.*, 111, D10304, doi:10.1029/2005JD006522, 2006.
- Weiss-Penzias, P., Jaffe, D. A., Swartzendruber, P., Hafner, W., Chand, D., and Prestbo, E.: Quantifying Asian and biomass burning sources of mercury using the Hg/CO ratio in pollution plumes observed at the Mount Bachelor Observatory, *Atmos. Environ.*, 41, doi:10.1016/j.atmosenv.2007.01.058, 2007.
- Wild, O. and Akimoto, H.: Intercontinental transport of ozone and its precursors in a three-dimensional global CTM, *J. Geophys. Res.*, 106, 27 729–27 744, 2001.
- Wolfe, G. M., Thornton, J. A., McNeill, V. F., Jaffe, D. A., Reidmiller, D., Chand, D., Smith, J., Swartzendruber, P., Flocke, F., and Zheng, W.: Influence of trans-Pacific pollution transport on acyl peroxy nitrate abundances and speciation at Mount Bachelor Observatory during INTEX-B, *Atmos. Chem. Phys.*, 7, 5309–5325, 2007, <http://www.atmos-chem-phys.net/7/5309/2007/>.
- Worden, J., Kulawik, S. S., Shephard, M. W., Clough, S. A., Worden, H., Bowman, K., and Goldman, A.: Predicted errors of tropospheric emission spectrometer nadir retrievals from spectral window selection, *J. Geophys. Res.*, 109, D09308, doi:10.1029/2004JD004522, 2004.
- Yienger, J. J. and Levy II, H.: Empirical model of global soil biogenic NO<sub>x</sub> emissions, *J. Geophys. Res.*, 100, 11 447–11 464, 1995.
- Yienger, J. J., Galanter, M., Holloway, T. A., Phadnis, M. J., Guttikunda, S. K., Carmichael, G. R., Moxim, W. J., and Levy, H.: The episodic nature of air pollution transport from Asia to North America, *J. Geophys. Res.*, 105, 26 931–26 945, 2000.
- Zhang, L., Jacob, D. J., Bowman, K. W., Logan, J. A., Turquety, S., Hudman, R. C., Li, Q., Beer, R., Worden, H. M., Worden, J. R., Rinsland, C. P., Kulawik, S. S., Lampel, M. C., Shephard, M. W., Fisher, B. M., Eldering, A., and Avery, M. A.: Continental outflow of ozone pollution as determined by O<sub>3</sub>-CO correlations from the TES satellite instrument, *Geophys. Res. Lett.*, 33, L18804, doi:10.1029/2006GL026399, 2006.
- Zhang, Q., Streets, D. G., He, K., Wang, Y., Richter, A., Burrows, J. P., Uno, I., Jang, C. J., Chen, D., Yao, Z., and Lei, Y.: NO<sub>x</sub> emission trends for China, 1995–2004: The view from the ground and the view from space, *J. Geophys. Res.*, 112, D22306, doi:10.1029/2007JD008684, 2007.

## Intercontinental source attribution of ozone pollution at western U.S. sites using an adjoint method

Lin Zhang,<sup>1</sup> Daniel J. Jacob,<sup>1,2</sup> Monika Kopacz,<sup>2</sup> Daven K. Henze,<sup>3</sup> Kumaresh Singh,<sup>4</sup> and Daniel A. Jaffe<sup>5</sup>

Received 27 February 2009; revised 23 April 2009; accepted 5 May 2009; published 6 June 2009.

[1] We use the GEOS-Chem chemical transport model and its adjoint to quantify source contributions to ozone pollution at two adjacent sites on the U.S. west coast in spring 2006: Mt. Bachelor Observatory (MBO) at 2.7 km altitude and Trinidad Head (TH) at sea level. The adjoint computes the sensitivity of ozone concentrations at the receptor sites to ozone production rates at  $2^\circ \times 2.5^\circ$  resolution over the history of air parcels reaching the site. MBO experiences distinct Asian ozone pollution episodes; most of the ozone production in these episodes takes place over East Asia with maxima over northeast China and southern Japan, adding to a diffuse background production distributed over the extratropical northern hemisphere. TH shows the same Asian origins for ozone as MBO but no distinct Asian pollution episodes. We find that transpacific pollution plumes transported in the free troposphere are diluted by a factor of 3 when entrained into the boundary layer, explaining why these plumes are undetectable in U.S. surface air. **Citation:** Zhang, L., D. J. Jacob, M. Kopacz, D. K. Henze, K. Singh, and D. A. Jaffe (2009), Intercontinental source attribution of ozone pollution at western U.S. sites using an adjoint method, *Geophys. Res. Lett.*, 36, L11810, doi:10.1029/2009GL037950.

### 1. Introduction

[2] Intercontinental transport of ozone pollution is becoming a major issue as countries at northern mid-latitudes strive to meet increasingly stringent air quality standards [*Task Force on Hemispheric Transport of Air Pollution*, 2007]. Ozone is produced in the troposphere by photochemical oxidation of CO and volatile organic compounds (VOCs) in the presence of nitrogen oxides ( $\text{NO}_x \equiv \text{NO} + \text{NO}_2$ ). It has a lifetime of days in the boundary layer but weeks in the free troposphere [*Wang et al.*, 1998], enabling transport on the intercontinental scale. Intercontinental source attribution for ozone pollution at a given site is made difficult by the complexity and non-linearity in the chemistry, the multiplicity of sources and time scales, and the general lack of structure of the ozone background

especially in surface air [*Goldstein et al.*, 2004]. We present here a new approach using the adjoint of a chemical transport model (CTM) and apply it to examine the detail of intercontinental influence on ozone pollution at two U.S. west coast sites.

[3] Previous CTM studies of intercontinental influence on surface ozone have used either ozone tracers tagged by production region [*Li et al.*, 2002; *Jaeglé et al.*, 2003; *Derwent et al.*, 2004; *Sudo and Akimoto*, 2007] or sensitivity simulations with perturbed emissions [*Jacob et al.*, 1999; *Yienger et al.*, 2000; *Wild and Akimoto*, 2001; *Derwent et al.*, 2008; *Duncan et al.*, 2008; *Fiore et al.*, 2009]. These source-oriented methods are computationally limited in the spatial resolution of the source region that they can achieve. The CTM adjoint offers a far more computationally efficient approach for a receptor-oriented problem such as source attribution of ozone at a given site. A single run of the adjoint model can compute the sensitivity of ozone concentrations at a given location and time (or an average over a spatial domain and time interval) to the global distribution of sources over the spatial and temporal resolution of the model. The method has been applied previously to pollutant transport to Hawaii [*Vukićević and Hess*, 2000; *Hess and Vukićević*, 2003], intercontinental transport of aerosol to the United States [*Henze et al.*, 2008], and regional sensitivity analyses for ozone pollution episodes [*Elbern and Schmidt*, 2001; *Hakami et al.*, 2006; *Nester and Panitz*, 2006].

[4] We use here the GEOS-Chem CTM and its adjoint to estimate source contributions to surface ozone pollution in spring 2006 at two nearby sites on the U.S. west coast, one at high altitude (Mt. Bachelor Observatory, Oregon) and one at sea level (Trinidad Head, California). The NASA/INTEX-B aircraft campaign over the northeast Pacific taking place at that time provided a detailed characterization of transpacific transport of ozone and its precursors [*Singh et al.*, 2009]. The GEOS-Chem simulation was previously evaluated in detail with INTEX-B as well as concurrent satellite and ground-based data, lending confidence in its representation of transpacific transport [*Zhang et al.*, 2008]. Mt. Bachelor Observatory and Trinidad Head are standard reference sites for background air entering the United States [*Goldstein et al.*, 2004; *Jaffe et al.*, 2005; *Oltmans et al.*, 2008]. The altitude difference between the two sites allows us to explore the dilution effect as Asian pollution plumes transported mainly in the free troposphere are entrained down to affect U.S. surface air.

### 2. GEOS-Chem Model and Its Adjoint

[5] The GEOS-Chem CTM (<http://www.as.harvard.edu/chemistry/trop/geos/>) [*Bey et al.*, 2001] is driven by assim-

<sup>1</sup>Department of Earth and Planetary Sciences, Harvard University, Cambridge, Massachusetts, USA.

<sup>2</sup>School of Engineering and Applied Sciences, Harvard University, Cambridge, Massachusetts, USA.

<sup>3</sup>Department of Mechanical Engineering, University of Colorado, Boulder, Colorado, USA.

<sup>4</sup>Department of Computer Science, Virginia Polytechnic Institute and State University, Blacksburg, Virginia, USA.

<sup>5</sup>Interdisciplinary Arts and Sciences, University of Washington Bothell, Bothell, Washington, USA.

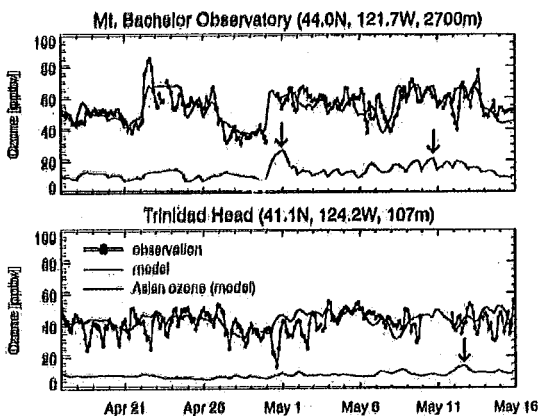


**Figure 1.** Time series of 3-hourly averaged ozone concentrations at (top) Mt. Bachelor Observatory and (bottom) Trinidad Head during the INTEX-B period (April 17–May 15, 2006). Model results (red) are compared to observations (black). The contribution of ozone produced over Asia in the model is also shown (blue). Black arrows indicate the Asian pollution events discussed in the text.

lated meteorological data from the Goddard Earth Observing System (GEOS)-4 of the NASA Global Modeling and Assimilation Office (GMAO). Details of its application to simulate satellite, aircraft, and ground-based observations of ozone and its precursors during INTEX-B (April 17–May 15, 2006) are given by Zhang *et al.* [2008]. The GEOS-4 dataset has a temporal resolution of 6 hours (3 hours for surface variables and mixing depths), a horizontal resolution of  $1^\circ \times 1.25^\circ$ , and 55 layers in the vertical. We degrade the horizontal resolution to  $2^\circ \times 2.5^\circ$  for input to GEOS-Chem. We use Asian anthropogenic emissions from Zhang *et al.* [2009] for the year 2006. U.S. anthropogenic emissions are from the National Emission Inventory for 1999 (NEI 99) by the U.S. Environmental Protection Agency (EPA) (<http://www.epa.gov/ttn/chieff/net/>). Transport of ozone from the stratosphere is simulated using the “Synoz” boundary condition of McLinden *et al.* [2000], which imposes a global cross-tropopause ozone flux of  $495 \text{ Tg a}^{-1}$ .

[6] Zhang *et al.* [2008] used a GEOS-Chem simulation with detailed  $\text{NO}_x$ -VOC chemistry for comparison to INTEX-B observations and for sensitivity analyses, but also archived daily 3-D fields of ozone production rates and loss frequencies to reproduce the ozone simulation results using tagged tracers of source regions. This tagged ozone tracer technique offers a computationally efficient approach for tracking the transport of ozone produced in different regions, and has been applied in a number of model studies [Wang *et al.*, 1998; Li *et al.*, 2002; Sudo and Akimoto, 2007]. We use it here in our adjoint model application. We define “Asian ozone” as ozone produced over Asia ( $8^\circ\text{N}$ – $55^\circ\text{N}$ ,  $70^\circ\text{E}$ – $152^\circ\text{E}$ ) throughout the tropospheric column. 80% of this production is in the lower troposphere below 700 hPa. Asian ozone defined in this way does not discriminate between anthropogenic and natural sources, nor does it quantitatively resolve ozone production from Asian precursors downwind of the continent. It assigns the source geographically rather than by precursor emissions. The

latter would be more precise for Asian anthropogenic source attribution but would require an adjoint model with full chemistry. Zhang *et al.* [2008] previously found by combining the two approaches that half of anthropogenic Asian influence on surface ozone in the western U.S. is from production in the Asian lower troposphere, with the rest from production in the free troposphere and downwind.

[7] The adjoint model of GEOS-Chem was constructed and tested by Henze *et al.* [2007] in work directed at constraining aerosol sources, and was further developed and applied by Kopacz *et al.* [2009] in an inverse analysis of CO emissions. We use the transport component of the adjoint including advection, boundary layer mixing, and convection [Henze *et al.*, 2007; K. Singh *et al.*, Towards the construction of a standard adjoint GEOS-Chem model, paper presented at High Performance Computing and Simulation Symposium, Soc. for Model. and Simul. Int., San Diego, Calif., 2009]. We add self-adjoint ozone chemistry with archived ozone production rates and loss frequencies. The resulting model is used to compute the sensitivity of ozone concentrations at selected receptor sites to 3-D ozone production rates at  $2^\circ \times 2.5^\circ$  resolution for different time lags and over the history of air parcels reaching the site.

### 3. Time Series of Ozone at U.S. West Coast Sites

[8] We use ozone measurements from Mt. Bachelor Observatory (MBO,  $44.0^\circ\text{N}$ ,  $121.7^\circ\text{W}$ , 2700 m) and Trinidad Head (TH,  $41.0^\circ\text{N}$ ,  $124.2^\circ\text{W}$ , 107 m). MBO is a mountain site in central Oregon that is particularly sensitive to Asian influences due to its exposure to the free troposphere [Jaffe *et al.*, 2005; Weiss-Penzias *et al.*, 2006; Wolfe *et al.*, 2007]. TH on the northern California coast is widely used as a surface background site for the United States [Goldstein *et al.*, 2004; Oltmans *et al.*, 2008; Parrish *et al.*, 2009]. The TH ozone measurements were obtained from <http://www.esrl.noaa.gov/gmd/obop/thd/>.

[9] Figure 1 shows the 3-hourly observed and modeled time series of ozone at MBO and TH for the INTEX-B period. There is good agreement between the measurements and GEOS-Chem. The mean observed concentration at MBO is  $54 \pm 10$  ppbv, compared with  $53 \pm 9$  ppbv in the model, while the mean observed concentration at TH is  $41 \pm 7$  ppbv, compared with  $43 \pm 5$  ppbv in the model. The model cannot reproduce the low ozone levels often observed at TH at night due to local deposition under stratified conditions [Goldstein *et al.*, 2004], but the synoptic-scale variability is well captured.

[10] The contribution of ozone produced over Asia in the model (“Asian ozone”) at the two sites is also shown in Figure 1. It averages  $13 \pm 3.6$  ppbv at MBO and  $8.4 \pm 1.4$  ppbv at TH. This is somewhat larger than the Asian anthropogenic ozone enhancement derived by Zhang *et al.* [2008] from a sensitivity simulation with Asian anthropogenic emissions turned off in the same model with full-chemistry ( $9 \pm 3$  ppbv at MBO). The difference is due to natural production over Asia contributing to Asian ozone as defined here; see section 2 for further discussion. The weaker and less variable contribution at TH than at MBO can be explained by dilution of free tropospheric plumes during entrainment in the boundary layer [Hudman *et al.*, 2004]. Model Asian ozone at MBO shows a maximum

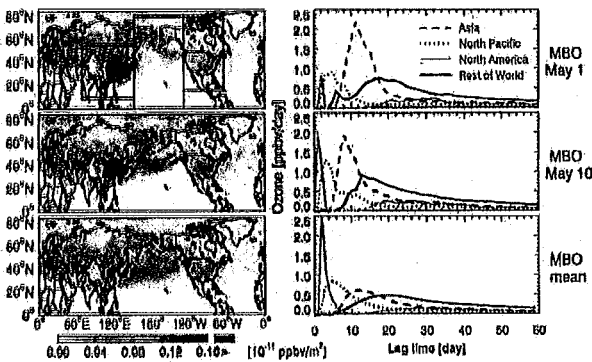


**Figure 2a.** Sensitivity of ozone concentrations at Mt. Bachelor Observatory, Oregon (MBO, 2.7 km altitude) to ozone production worldwide as inferred from the GEOS-Chem adjoint model: Asian pollution events at MBO ((top) May 1, 2006, at 00 UT and (middle) May 10, 2006, at 18 UT) as highlighted in Figure 1 and (bottom) the mean for the INTEX-B period (April 17–May 15, 2006). (left) The sensitivities integrated in time, over the depth of the tropospheric column and at the  $2^\circ \times 2.5^\circ$  grid resolution of the model. (right) The time-dependent sensitivities (going back in time) to ozone production over Asia, the North Pacific, North America, and Rest of World (as indicated by rectangles).

event on May 1 (26 ppbv) and a broader event on May 6–11, consistent with independent analyses of Asian pollution plumes observed at MBO during INTEX-B [Wolfe *et al.*, 2007; Zhang *et al.*, 2008]. Asian ozone at TH shows maximum influence on May 12, reflecting subsidence of the May 6–11 MBO plumes.

#### 4. Fine Geographical Source Attribution for Ozone

[11] Figure 2 shows the sensitivities of ozone concentrations at MBO and TH to the global distribution of ozone production rates for the previous two months, as inferred from the GEOS-Chem model adjoint. The left panels show the integrals of the production rates over time and over the tropospheric column depths at the  $2^\circ \times 2.5^\circ$  horizontal resolution of the model. They show the amount of ozone produced in each grid square and transported to the receptor site with chemical loss accounted for during transport. Summing these values globally over all  $2^\circ \times 2.5^\circ$  grid squares approximates the ozone concentrations simulated by GEOS-Chem at the receptor site; there is a 10%–15% residual that reflects production in the stratosphere and tropospheric production at time lags larger than 2 months. The right panels show the time-dependent sensitivities to production over Asia ( $8^\circ\text{N}$ – $55^\circ\text{N}$ ,  $70^\circ\text{E}$ – $152^\circ\text{E}$ ), North Pacific ( $0^\circ\text{N}$ – $80^\circ\text{N}$ ,  $152^\circ\text{E}$ – $232^\circ\text{W}$ ), North America ( $15^\circ\text{N}$ – $80^\circ\text{N}$ ,  $232^\circ\text{W}$ – $295^\circ\text{W}$ ), and Rest of World. Similar sensitivity spectra have been shown by Vukićević and Hess [2000]. Integrating under these curves gives the total contributions of ozone production in these regions to the ozone concentrations at the receptor site.

#### 4.1. Asian Pollution Events

[12] Figure 2a (top) show the sensitivities of ozone concentrations at MBO for the transpacific ozone pollution events of May 1 at 00 UT and May 10 at 18 UT. Most of the ozone production contributing to MBO ozone on these days took place over East Asia, with maxima over the northeast China plain and southern Japan. We also find significant production over the North Pacific during plume transport. The May 1 plume took a more northerly and higher-altitude route than the May 10 plume, resulting in less ozone production over the Pacific [Zhang *et al.*, 2008]. Both plumes show a secondary maximum of ozone production just off the west coast of United States, where subsidence of air masses causes decomposition of Asian PAN (peroxyacetylnitrate, a thermo-unstable  $\text{NO}_x$  reservoir species) and drives further ozone production [Kotchenruther *et al.*, 2001; Heald *et al.*, 2003; Hudman *et al.*, 2004; Zhang *et al.*, 2008]. In addition to these direct Asian pollution influences, both plumes show a significant background contribution to ozone from diffuse production in the extratropical northern hemisphere.

[13] The sensitivity spectra on Figures 2a (right) and 2b (right) show the transport timescales from production region to the receptor site. We see for the two Asian pollution episodes (top two panels) that ozone produced over North America had an immediate impact on MBO; this mostly reflects the decomposition of PAN in the subsiding air mass as discussed above rather than North American emissions. The North American contribution also shows a weak secondary peak at 20 days that reflects ozone produced in the United States and transported in the westerly atmospheric circulation.

[14] We find that ozone production over Asia begins to impact MBO after a 6-day time lag and that maximum Asian influence for the two events is at time lags of 8–11 days. This is consistent with previous studies showing that Asian pollution plumes can be transported across the Pacific in 5–10 days [Ylenger *et al.*, 2000; Stahl *et al.*, 2002]. We related these time lags to observed cold front passages over eastern Asia on April 21 and May 3, lifting Asian pollution in warm conveyor belts (WCBs) that enables rapid transport across the Pacific [Liu *et al.*, 2003]. The Asian sensitivity spectra also show a long tail, similar to the North American spectra and indicating the impact on background ozone in addition to direct transport.

[15] The May 12 event at TH (Figure 2b, top) shows similar source attribution as the May 10 event at MBO and

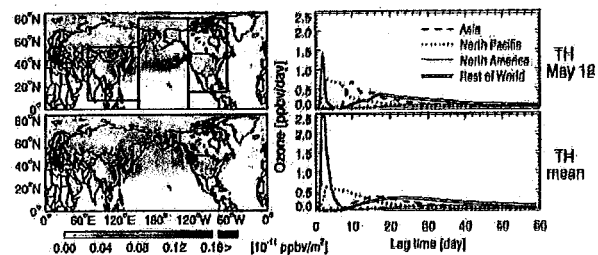


**Figure 2b.** Same as Figure 2a, but for Trinidad Head, California (TH, sea level). The event is for May 12, 2006, at 15 UT.

can be interpreted as subsidence of the free tropospheric plume that affected MBO on May 6–11. The Asian influence is much weaker at TH. Its sensitivity spectrum peaks at a time lag of 10 days, 2 day after that at MBO. Integrating the Asian sensitivity spectra for the events at MBO and TH over time lags of 5–20 days (direct transport component as opposed to background), we find a factor of 3 dilution effect as the plume mixes down to the surface (15 ppbv at MBO vs. 5 ppbv at TH). Hudman *et al.* [2004] previously estimated a factor of 10 dilution between the free troposphere and surface air for Asian dust plumes observed over the western United States.

#### 4.2. Mean Conditions at MBO and TH

[16] Figure 2a (bottom) shows the source attribution for the mean ozone concentration at MBO during the INTEX-B period. The patterns are similar to the Asian pollution events previously discussed but the influence of direct Asian transport is weaker. Background production is mainly north of 20°N. Fine structure in the contributions from source regions in Asia can still clearly be distinguished, with maximum contributions from eastern China (5 ppbv) and Japan (1 ppbv) as derived by summing the corresponding grid squares. The Japanese contribution as identified from the adjoint model is mainly from boundary layer production and hence associated with local anthropogenic emissions. Its contribution to transpacific pollution to the U.S. is higher than would be expected from its NO<sub>x</sub> emissions (0.7 Tg N a<sup>-1</sup>) relative to China (6.4 Tg N a<sup>-1</sup>) [Zhang *et al.*, 2009]. Export of Japanese pollutants into the westerly flow of the North Pacific is more efficient than for China [Wild *et al.*, 2004]. The mean ozone concentration at MBO is also sensitive to sustained production over the North Pacific from Asian pollution at 25°N–40°N, and particularly off the North American west coast, as previously discussed by Zhang *et al.* [2008].

[17] Figure 2b shows the sensitivity of the mean ozone concentration at Trinidad Head to production upwind. North American production is more important than at MBO. Asian influence is weaker than at MBO but still shows the Eastern China – southern Japan dipole. Asian ozone by summing the sensitivities over Asia is 8 ppbv at TH, consistent with studies using source-oriented methods [Jaeglé *et al.*, 2003; Goldstein *et al.*, 2004; Zhang *et al.*, 2008]. The peak in Asian influence is at a time lag of 16 days, as compared to 12 days at MBO, reflecting the delay and dilution during entrainment from the free troposphere to the surface. The mean transport time from Asia, calculated as the sensitivity-weighted mean time lag [Vukićević and Hess, 2000], is 23 days for MBO and 27 days for TH, comparable to the mean transport time of 2–3 weeks from East Asia to the western North America surface previously estimated by Liu and Mauzerall [2005].

[18] In summary, we have shown that an adjoint model analysis can provide detailed geographical and temporal information on intercontinental pollution influences at specific receptor sites. Such information can be used to better determine the sources of this intercontinental pollution, down to the scale of individual source countries and urban areas. For policy purposes it will be important to attribute intercontinental ozone pollution to the actual emissions of ozone precursors, in particular NO<sub>x</sub>, taking advantage of the

fine resolution enabled by the adjoint. This requires an adjoint of the model chemical mechanism to resolve the non-linearity on ozone production and hence a more elaborate calculation than was presented here.

[19] **Acknowledgments.** This work was funded by the NASA Atmospheric Chemistry Modeling and Analysis Program and by NASA Headquarters under the Earth and Space Science Fellowship Program Grant NNX07AN65H to Lin Zhang.

#### References

- Bey, I., D. J. Jacob, R. M. Yantosca, J. A. Logan, B. D. Field, A. M. Fiore, Q. Li, H. Y. Liu, L. J. Mielke, and M. G. Schultz (2001), Global modeling of tropospheric chemistry with assimilated meteorology: Model description and evaluation, *J. Geophys. Res.*, **106**, 23,073–23,095.
- Derwent, R. G., D. S. Stevenson, W. J. Collins, and C. E. Johnson (2004), Intercontinental transport and the origins of the ozone observed at surface sites in Europe, *Atmos. Environ.*, **38**, 1891–1901.
- Derwent, R. G., et al. (2008), How is surface ozone in Europe linked to Asian and North American NO<sub>x</sub> emissions?, *Atmos. Environ.*, **42**, 7412–7422.
- Duncan, B. N., J. J. West, Y. Yoshida, A. M. Fiore, and J. R. Ziemke (2008), The influence of European pollution on ozone in the Near East and northern Africa, *Atmos. Chem. Phys.*, **8**, 2267–2283.
- Elbern, H., and H. Schmidt (2001), Ozone episode analysis by four-dimensional variational chemistry data assimilation, *J. Geophys. Res.*, **106**, 3569–3590.
- Fiore, A. M., et al. (2009), Multi-model estimates of intercontinental source-receptor relationships for ozone pollution, *J. Geophys. Res.*, **114**, D04301, doi:10.1029/2008JD010816.
- Goldstein, A. H., D. B. Millet, M. McKay, L. Jaeglé, L. Horowitz, O. Cooper, R. Hudman, D. J. Jacob, S. Oltmans, and A. Clarke (2004), Impact of Asian emissions on observations at Trinidad Head, California, during ITCT 2K2, *J. Geophys. Res.*, **109**, D23S17, doi:10.1029/2003JD004406.
- Hakami, A., et al. (2006), Adjoint sensitivity analysis of ozone nonattainment over the continental United States, *Environ. Sci. Technol.*, **40**, 3855–3864.
- Heald, C. L., et al. (2003), Asian outflow and transpacific transport of carbon monoxide and ozone pollution: An integrated satellite, aircraft, and model perspective, *J. Geophys. Res.*, **108**(D24), 4804, doi:10.1029/2003JD003507.
- Henze, D. K., A. Hakami, and J. H. Seinfeld (2007), Development of the adjoint of GEOS-Chem, *Atmos. Chem. Phys.*, **7**, 2413–2433.
- Henze, D. K., D. T. Shindell, and J. H. Seinfeld (2008), Inverse modeling and mapping US air quality influences of inorganic PM<sub>2.5</sub> precursor emissions using the adjoint of GEOS-Chem, *Atmos. Chem. Phys. Discuss.*, **8**, 15,033–15,099.
- Hess, P. G., and T. Vukićević (2003), Intercontinental transport, chemical transformations, and baroclinic systems, *J. Geophys. Res.*, **108**(D12), 4354, doi:10.1029/2002JD002798.
- Hudman, R. C., et al. (2004), Ozone production in transpacific Asian pollution plumes and implications for ozone air quality in California, *J. Geophys. Res.*, **109**, D23S10, doi:10.1029/2004JD004974.
- Jacob, D. J., J. A. Logan, and P. P. Mutt (1999), Effect of rising emissions on surface ozone in the United States, *Geophys. Res. Lett.*, **26**, 2175–2178.
- Jaeglé, L., D. A. Jaffe, H. U. Price, P. Weiss-Penzias, P. I. Palmer, M. J. Evans, D. J. Jacob, and I. Bey (2003), Sources and budgets for CO and O<sub>3</sub> in the northeastern Pacific during the spring of 2001: Results from the PHOBEA-II Experiment, *J. Geophys. Res.*, **108**(D20), 8802, doi:10.1029/2002JD003121.
- Jaffe, D., et al. (2005), Export of atmospheric mercury from Asia, *Atmos. Environ.*, **39**, 3029–3038.
- Kopacz, M., D. J. Jacob, D. K. Henze, C. L. Heald, D. G. Streets, and Q. Zhang (2009), Comparison of adjoint and analytical Bayesian inversion methods for constraining Asian sources of carbon monoxide using satellite (MOPITT) measurements of CO columns, *J. Geophys. Res.*, **114**, D04305, doi:10.1029/2007JD009264.
- Kotchenruther, R. A., D. A. Jaffe, and L. Jaeglé (2001), Ozone photochemistry and the role of PAN in the springtime northeastern Pacific troposphere: Results from the PHOBEA campaign, *J. Geophys. Res.*, **106**, 28,731–28,741.
- Li, Q., et al. (2002), Transatlantic transport of pollution and its effects on surface ozone in Europe and North America, *J. Geophys. Res.*, **107**(D13), 4166, doi:10.1029/2001JD001422.
- Liu, H., D. J. Jacob, I. Bey, R. M. Yantosca, B. N. Duncan, and G. W. Sachse (2003), Transport pathways for Asian combustion outflow over

- the Pacific: Interannual and seasonal variations, *J. Geophys. Res.*, *108*(D20), 8786, doi:10.1029/2002JD003102.
- Liu, J., and D. L. Mauzerall (2005), Estimating the average time for intercontinental transport of air pollutants, *Geophys. Res. Lett.*, *32*, L11814, doi:10.1029/2005GL022619.
- McLinden, C. A., S. C. Olsen, B. Hannegan, O. Wild, M. J. Prather, and J. Sundet (2000), Stratospheric ozone in 3-D models: A simple chemistry and the cross-tropopause flux, *J. Geophys. Res.*, *105*, 14,653–14,665.
- Nester, K., and H.-J. Panitz (2006), Sensitivity analysis by the adjoint chemistry transport model DRAIS for an episode in the Berlin Ozone (BERLIOZ) experiment, *Atmos. Chem. Phys.*, *6*, 2091–2106.
- Oltmans, S. J., et al. (2008), Background ozone levels of air entering the west coast of the US and assessment of longer-term changes, *Atmos. Environ.*, *42*, 6020–6038.
- Parrish, D. D., D. B. Millet, and A. H. Goldstein (2009), Increasing ozone in marine boundary layer inflow at the west coasts of North America and Europe, *Atmos. Chem. Phys.*, *9*, 1303–1323.
- Singh, H. B., W. H. Brune, J. H. Crawford, F. Flocke, and D. J. Jacob (2009), Chemistry and transport of pollution over the Gulf of Mexico and the Pacific: Spring 2006 INTEX-B Campaign overview and first results, *Atmos. Chem. Phys. Discuss.*, *9*, 363–409.
- Stohl, A., S. Eckhardt, C. Forster, P. James, and N. Spichtinger (2002), On the pathways and timescales of intercontinental air pollution transport, *J. Geophys. Res.*, *107*(D23), 4684, doi:10.1029/2001JD001396.
- Sudo, K., and H. Akimoto (2007), Global source attribution of tropospheric ozone: Long-range transport from various source regions, *J. Geophys. Res.*, *112*, D12302, doi:10.1029/2006JD007992.
- Task Force on Hemispheric Transport of Air Pollution (2007), 2007 interim report, Geneva, Switzerland. (Available at [www.htap.org](http://www.htap.org))
- Vukićević, T., and P. Hess (2000), Analysis of tropospheric transport in the Pacific Basin using the adjoint technique, *J. Geophys. Res.*, *105*, 7213–7230.
- Wang, Y., D. J. Jacob, and J. A. Logan (1998), Global simulation of tropospheric O<sub>3</sub>-NO<sub>x</sub>-hydrocarbon chemistry: 3. Origin of tropospheric ozone and effects of non-methane hydrocarbons, *J. Geophys. Res.*, *103*, 10,757–10,768.
- Weiss-Penzias, P., D. A. Jaffe, P. Swartzendruber, J. B. Dennison, D. Chand, W. Hafner, and E. Prestbo (2006), Observations of Asian air pollution in the free troposphere at Mount Bachelor Observatory during the spring of 2004, *J. Geophys. Res.*, *111*, D10304, doi:10.1029/2005JD006522.
- Wild, O., and H. Akimoto (2001), Intercontinental transport of ozone and its precursors in a three dimensional globe CTM, *J. Geophys. Res.*, *106*, 27,729–27,744.
- Wild, O., et al. (2004), Chemical transport model ozone simulations for spring 2001 over the western Pacific: Regional ozone production and its global impacts, *J. Geophys. Res.*, *109*, D15S02, doi:10.1029/2003JD004041.
- Wolfe, G. M., et al. (2007), Influence of trans-Pacific pollution transport on acyl peroxy nitrate abundances and speciation at Mount Bachelor Observatory during INTEX-B, *Atmos. Chem. Phys.*, *7*, 5309–5325.
- Yienger, J. J., M. Galanter, T. A. Holloway, M. J. Phadnis, S. K. Guttikunda, G. R. Carmichael, W. J. Moxim, and H. Levy II (2000), The episodic nature of air pollution transport from Asia to North America, *J. Geophys. Res.*, *105*, 26,931–26,945.
- Zhang, L., et al. (2008), Transpacific transport of ozone pollution and the effect of recent Asian emission increases on air quality in North America: An integrated analysis using satellite, aircraft, ozonesonde, and surface observations, *Atmos. Chem. Phys.*, *8*, 6117–6136.
- Zhang, Q., et al. (2009), Asian emissions in 2006 for the NASA INTEX-B mission, *Atmos. Chem. Phys. Discuss.*, *9*, 4081–4139.

D. K. Henze, Department of Mechanical Engineering, University of Colorado, Boulder, CO 80309, USA.

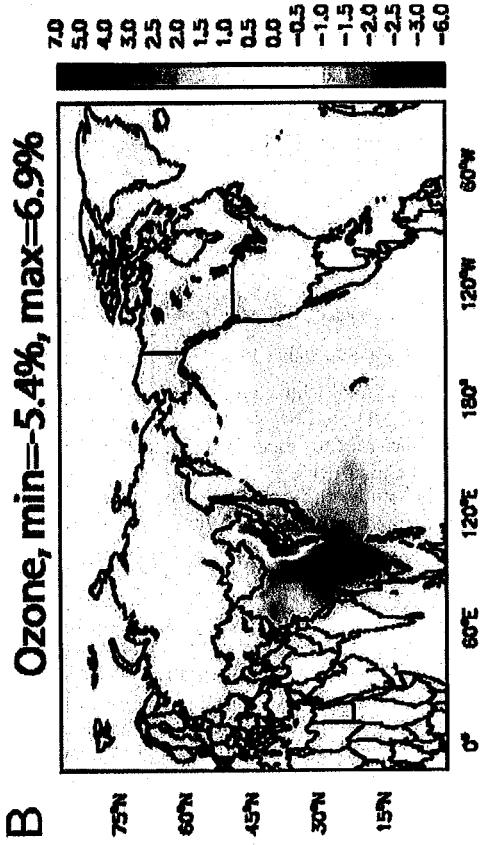
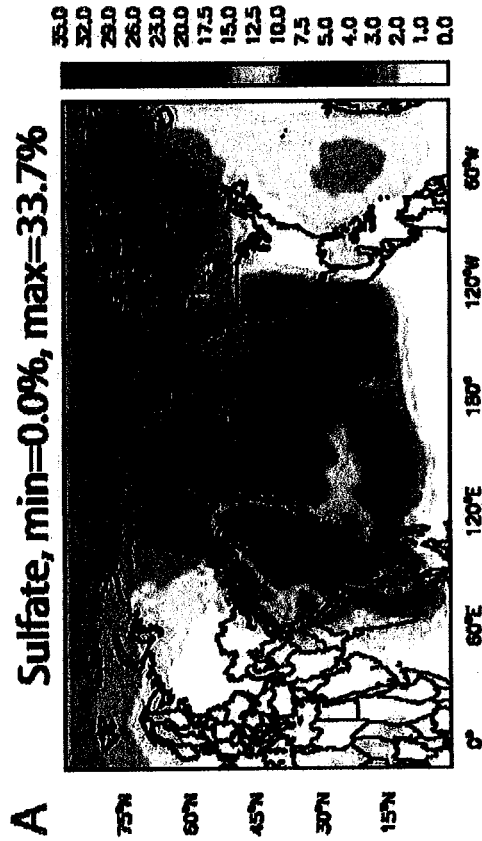
D. J. Jacob and L. Zhang, Department of Earth and Planetary Sciences, Harvard University, Cambridge, MA 02138, USA. ([linzhang@fas.harvard.edu](mailto:linzhang@fas.harvard.edu))

D. A. Jaffe, Interdisciplinary Arts and Sciences, University of Washington Bothell, Bothell, WA 98011–8246, USA.

M. Kopacz, School of Engineering and Applied Sciences, Harvard University, Cambridge, MA 02138, USA.

K. Singh, Department of Computer Science, Virginia Polytechnic Institute and State University, Blacksburg, VA 24060, USA.

**Simulated percentage contribution of surface air pollution in 2006 from Chinese EEE for (A) sulfate, (B) ozone, (C) BC, and (D) CO. Results are shown for annual mean concentrations in the lowest model layer (0–130 m), presented as (simulation 1 – simulation...**



Jintai Lin et al. PNAS 2014;111:1736-1741

# China's international trade and air pollution in the United States

Jintal Lin<sup>a,1,2</sup>, Da Pan<sup>a,1</sup>, Steven J. Davis<sup>b</sup>, Qiang Zhang<sup>c,2</sup>, Kebin He<sup>d,e,2</sup>, Can Wang<sup>c,d</sup>, David G. Streets<sup>f</sup>, Donald J. Wuebbles<sup>g</sup>, and Dabo Guan<sup>c,h</sup>

<sup>a</sup>Laboratory for Climate and Ocean-Atmosphere Studies, Department of Atmospheric and Oceanic Sciences, School of Physics, Peking University, Beijing 100871, China; <sup>b</sup>Department of Earth System Science, University of California, Irvine, CA 92697; <sup>c</sup>Ministry of Education Key Laboratory for Earth System Modelling, Center for Earth System Science, Tsinghua University, Beijing 100084, China; <sup>d</sup>State Key Joint Laboratory of Environmental Simulation and Pollution Control, School of Environment, Tsinghua University, Beijing 100084, China; <sup>e</sup>Collaborative Innovation Center for Regional Environmental Quality, Beijing 100084, China; <sup>f</sup>Argonne National Laboratory, Lemont, IL 60439; <sup>g</sup>Department of Atmospheric Sciences, School of Earth, Society, and Environment, University of Illinois at Urbana-Champaign, Urbana, IL 61801; and <sup>h</sup>water@leeds, School of Earth and Environment, University of Leeds, Leeds, LS2 9JT, United Kingdom

Edited by Dan Jaffe, University of Washington, Seattle, WA, and accepted by the Editorial Board December 18, 2013 (received for review July 10, 2013)

China is the world's largest emitter of anthropogenic air pollutants, and measurable amounts of Chinese pollution are transported via the atmosphere to other countries, including the United States. However, a large fraction of Chinese emissions is due to manufacture of goods for foreign consumption. Here, we analyze the impacts of trade-related Chinese air pollutant emissions on the global atmospheric environment, linking an economic-emission analysis and atmospheric chemical transport modeling. We find that in 2006, 36% of anthropogenic sulfur dioxide, 27% of nitrogen oxides, 22% of carbon monoxide, and 17% of black carbon emitted in China were associated with production of goods for export. For each of these pollutants, about 21% of export-related Chinese emissions were attributed to China-to-US export. Atmospheric modeling shows that transport of the export-related Chinese pollution contributed 3–10% of annual mean surface sulfate concentrations and 0.5–1.5% of ozone over the western United States in 2006. This Chinese pollution also resulted in one extra day or more of noncompliance with the US ozone standard in 2006 over the Los Angeles area and many regions in the eastern United States. On a daily basis, the export-related Chinese pollution contributed, at a maximum, 12–24% of sulfate concentrations over the western United States. As the United States outsourced manufacturing to China, sulfate pollution in 2006 increased in the western United States but decreased in the eastern United States, reflecting the competing effect between enhanced transport of Chinese pollution and reduced US emissions. Our findings are relevant to international efforts to reduce transboundary air pollution.

Input-output analysis | emission control | international collaboration

A key driver of the rapid economic growth in China over the past decade is the great expansion in the production of goods for export (1). Although growth has slowed since the global financial crisis, between 2000 and 2007 the volume of Chinese exports grew by 390% (2). As the Chinese economy has grown, the economic structure has also changed, transitioning from a net importer to a large net exporter of energy-intensive industrial products (2). The energy needed to support this economic growth and transformation has come from combustion of fossil fuels, primarily coal, which has contributed to a global increase in emissions of carbon dioxide (CO<sub>2</sub>) (3, 4). At the same time, increased combustion of fossil fuels, relatively low combustion efficiency, and weak emission control measures have also led to drastic increases in air pollutants such as sulfur dioxide (SO<sub>2</sub>), nitrogen oxides (NO<sub>x</sub>), carbon monoxide (CO), black carbon (BC), and primary organic carbon (OC) (5–8). Indeed, fossil-fuel-intensive manufacturing, large manufacturing volume, and relatively weak emission controls have meant that China emits far more pollutants per unit of gross domestic product (GDP) than countries with more advanced industrial and emission control technologies (SI Appendix, Table S1). Per unit

of GDP in 2006, China emitted 6–33 times as much air pollutants as the United States (Fig. 1 E–H). For these reasons, air quality has recently become a major focus of environmental policy in China (8).

In this study, the terms “export,” “import,” and “trade” all refer to transaction of goods between countries. The pollutants emitted in China due to its production of goods for foreign consumption are regarded as emissions embodied in export (EEE) of China (9, 10). The EEE is unique in that the associated goods are consumed outside of China, raising a question about the extent to which China and its export partners should be accountable for the emissions (10–12). The attribution depends on whether the emission accounting is based on production or on consumption. Production-based accounting considers all emissions physically produced in China to be Chinese emissions, including the EEE. Such accounting is used as default in current emission inventories such as the Emission Database for Global Atmospheric Research (13). By comparison, consumption-based accounting views all emissions associated with production of goods consumed by China to be China's responsibility, no matter whether the production occurs in China or in other countries (9, 10). Thus, the consumption-based Chinese emissions exclude the EEE but include the emissions embodied in import of China

## Significance

International trade affects global air pollution and transport by redistributing emissions related to production of goods and services and by potentially altering the total amount of global emissions. Here we analyze the trade influences by combining an economic-emission analysis on China's bilateral trade and atmospheric chemical transport modeling. Our focused analysis on US air quality shows that Chinese air pollution related to production for exports contributes, at a maximum on a daily basis, 12–24% of sulfate pollution over the western United States. The US outsourcing of manufacturing to China might have reduced air quality in the western United States with an improvement in the east, due to the combined effects of changes in emissions and atmospheric transport.

Author contributions: J.L., Q.Z., K.H., and D.G. designed research; J.L. and D.P. performed research; J.L., D.P., S.J.D., Q.Z., K.H., C.W., D.G.S., D.J.W., and D.G. analyzed data; and J.L., D.P., S.J.D., Q.Z., K.H., C.W., D.G.S., D.J.W., and D.G. wrote the paper.

The authors declare no conflict of interest.

This article is a PNAS Direct Submission. D.J. is a guest editor invited by the Editorial Board.

Freely available online through the PNAS open access option.

<sup>1</sup>J.L. and D.P. contributed equally to this work.

<sup>2</sup>To whom correspondence may be addressed. E-mail: jintal@pku.edu.cn, qiangzhang@tsinghua.edu.cn, or hekb@tsinghua.edu.cn.

This article contains supporting information online at [www.pnas.org/lookup/suppl/doi:10.1073/pnas.1312860111/-DCSupplemental](http://www.pnas.org/lookup/suppl/doi:10.1073/pnas.1312860111/-DCSupplemental).

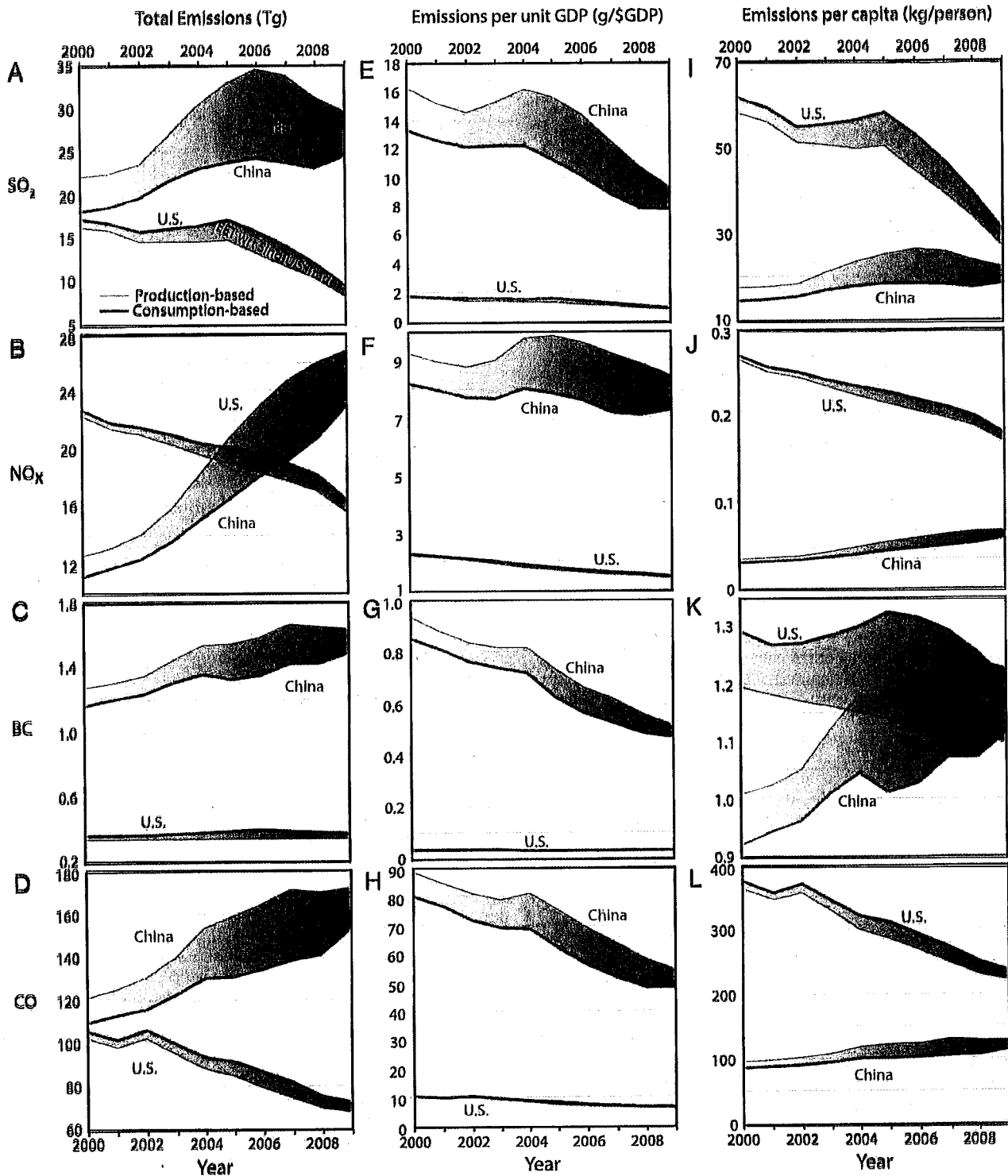


**Fig. 1.** Air pollutants embodied in Chinese trade between 2000 and 2009. (A–D) Production-based emissions (thin lines), consumption-based emissions (thick lines), and their differences (i.e., Chinese EET associated with its trade with the rest of the world in purple shading, and EET associated with Sino-US trade alone in green shading). All Chinese emissions are calculated here, the US production-based emissions are taken from the National Emissions Inventory, and the US consumption-based emissions are derived based on production-based emissions and Sino-US trade-related emissions. Although China's production-based emissions are growing rapidly, its EET are equivalent to substantial fractions of the production-based emissions. Similarly, the EET due to Sino-US trade are equivalent to large proportions of the production-based US emissions since 2006. (E–H) Emissions per GDP. Although China's production-based emissions per unit GDP have been decreasing, its consumption-based emissions per unit GDP have decreased less significantly or have increased since 2008. (I–L) Emissions per capita. Per capita emissions are very different between the United States and China, and this disparity is increased when the consumption-based emissions are considered. For data sources, see *S1 Appendix*, Table S1, footnote.

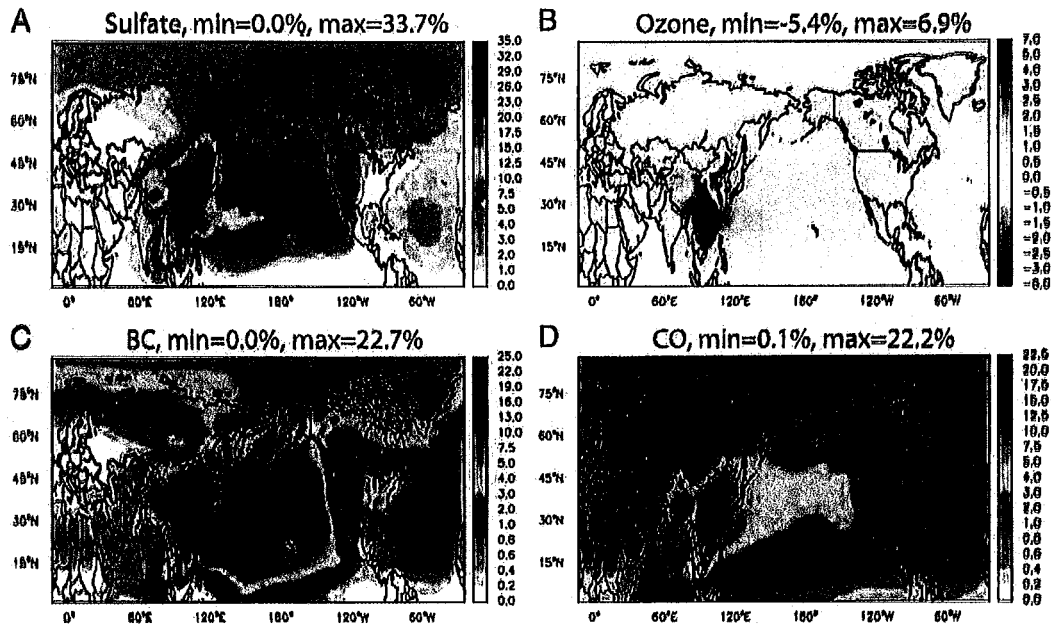


**Fig. 2.** Simulated percentage contribution of surface air pollution in 2006 from Chinese EEE for (A) sulfate, (B) ozone, (C) BC, and (D) CO. Results are shown for annual mean concentrations in the lowest model layer (0–130 m), presented as (simulation 1 – simulation 2)/simulation 1 in the *SI Appendix*, section 6. The color scale is nonlinear to better present the wide range of impacts over different regions. The Chinese EEE affect pollutant concentrations most significantly over China, but they also affect the rest of East Asia, the Arctic, western North America, and other regions downwind of China. The negative impacts on ozone concentrations over parts of the northern Chinese provinces are primarily because the EEE-related  $\text{NO}_x$  emissions increase the ozone sink in the nighttime overcompensating for the effect of enhanced ozone production in the daytime.

(EEI, i.e., emissions in other countries due to production of goods for Chinese consumption). The numerical difference between production- and consumption-based emissions of China is the EEI less the EEI, the result of which is regarded as the emissions embodied in net trade (EET) of China (10). Similar emission analyses are applicable to other countries.

Previous studies have quantified the substantial  $\text{CO}_2$  emissions embodied in Chinese trade (10, 11). Thus, far, however, relatively little attention has been paid to trade-related emissions of short-lived air pollutants and especially the resulting impacts on the global atmospheric environment, except for an analysis done for local air quality of the Pearl River Delta (14). This is true despite the direct harm these pollutants do to human health (15–18), agriculture (19), ecosystems (20), and global climate (21, 22). And as scientific evidence of transport of Chinese air pollution across the Pacific Ocean has grown since the late 1990s (23–29), the United States and Canada have a special interest in reducing Chinese air pollution. In the case of  $\text{CO}_2$ , consumption-based accounting of emissions has been motivated by the argument—often made by developing countries—that consumers who benefit from a process should bear some responsibility for associated environmental damage (30). A similar accounting for emissions of air pollutants and consequent impacts on the global atmospheric environment may therefore be necessary to facilitate discussion of international collaborations on transboundary air pollution control (31).

We quantify the emissions of  $\text{SO}_2$ ,  $\text{NO}_x$ , CO, BC, and OC embodied in Chinese exports and imports between 2000 and 2009 using an economic input-output model constructed from economic and emission data. The model resolves trade between China and four countries/regions [the United States, the European Union (EU), Japan, and an aggregated region of all other countries] and 42 industry sectors, and allocates pollutant emissions to countries and industry sectors according to where goods are consumed. As part of our analysis, we also quantify the

uncertainties in emission derivation using a Monte Carlo approach. We then simulate the effects of export-related Chinese emissions on air pollution in China and downwind regions, using the GEOS-Chem global chemical transport model. See *SI Appendix* for details of our analytic approach, data sources, and model simulations.

## Results

Fig. 1 A–D shows the trends over 2000–2009 in the EET of China related to its trade with the rest of the world (purple shading) and in the EET with respect to Sino-US trade alone (green shading), together with the production- and consumption-based emission accounting for China and the United States. For China, although the production-based emissions of  $\text{SO}_2$  and BC have declined since 2007 due to the global financial crisis and sulfur emission control, the consumption-based emissions of all pollutants have continued to rise, reflecting a net decrease in the EET. Nonetheless, the EET were equivalent to a large fraction of production-based Chinese emissions, and this fraction expanded between 2000 and 2006. For example, the EET of  $\text{SO}_2$  grew from 4.0 teragrams (Tg) (equivalent to 18% of production-based Chinese emissions) in 2000 to 10.3 Tg (30%) in 2006 (Fig. 1A). The fraction of the EET grew similarly for  $\text{NO}_x$ , CO, and BC (Fig. 1 B–D). Meanwhile, although the EET for Sino-US trade were equivalent only to 2–8% of production-based US emissions in 2000, the proportion grew by a factor of 2–3 to reach 6–19% in 2006 (Fig. 1 A–D). This trend reflects the decline of production-based emissions of the United States and its continuous outsourcing (32).

Although the EET represent the difference between the EEI and the EEI, the EET of China were numerically close to its EEI over 2000–2009. This is because the EEI of China are larger than the EEI by a factor of 4–6 during these years, reflecting China's trade imbalance with the rest of the world, the types of goods being traded, and the differences in emission intensity between China and its trading partners (*SI Appendix*,

section 5.2). In 2006, the Chinese EEE contributed 36% of its production-based emissions for  $\text{SO}_2$ , 27% for  $\text{NO}_x$ , 22% for CO, and 17% for BC. And for all these pollutants, about 21% of the Chinese EEE in 2006 were attributed to China-to-US export of goods.

Fig. 1 E–H shows that Chinese emissions per unit of GDP have mostly decreased between 2000 and 2009. However, the production-based emissions per unit GDP have recently decreased at a faster rate than have the consumption-based emissions per unit GDP. In the case of  $\text{NO}_x$ , the consumption-based Chinese emissions per unit GDP have actually increased since 2008 (Fig. 1F). Meanwhile, emissions per unit GDP have also declined in the United States, regardless of whether or not the emissions embodied in Sino-US trade are included (Fig. 1 E–H). The emissions per unit GDP for China are much greater than those for the United States, based on both production- and consumption-based accounting. In 2009, the production-based emissions per unit GDP for China were about 6–17 times greater than the United States. The difference in consumption-based emissions per unit GDP was somewhat less; 5–14 times greater in China than the United States.

Finally, Fig. 1 I–L illustrates the large gap in emissions per capita between the United States and China. Over 2000–2009, the EET per capita for China related to its trade with the rest of the world (purple shading) were close to the EET per capita for the United States related to Sino-US trade alone (green shading). For China, although the production-based emissions per capita have fallen or flattened since 2007, the consumption-based emissions per capita have increased (Fig. 1 I–L). This again suggests that the global financial crisis affected Chinese exports but did not stem domestic growth. The trends contrast to the reductions in both production- and consumption-based emissions per capita for the United States.

Using the GEOS-Chem chemical transport model, we simulated the impacts of the EEE-related Chinese pollution on the global atmospheric environment in 2006 (SI Appendix, section 6 for descriptions of various model simulations). Fig. 2 shows the modeled percentage of annual mean surface pollutant concentrations in the Northern Hemisphere in 2006 attributable to the atmospheric transport and transformation of the EEE-related Chinese air pollution. The EEE-related Chinese pollution accounted for 23–34% of sulfate concentrations, 10–23% of BC, and 12–23% of CO over East China (east of  $100^\circ\text{E}$ ). This pollution resulted in ozone reductions over the North China Plain and Northeast China with ozone enhancements over the southern provinces. The mixed impacts reflect the nonlinear chemical processes that govern the ozone level: The additional  $\text{NO}_x$  due to Chinese EEE enhanced the nighttime ozone loss, compensating for the effect of enhanced daytime ozone production (33).

Fig. 2 shows that, through the atmospheric transport and transformation, parts of the EEE-related Chinese pollution in 2006 affected the surface air pollutant levels over the rest of East Asia, the North Pacific, western North America, Arctic, and other regions downwind of China. In particular, the EEE-related Chinese pollution contributed about 3–10% of the annual mean surface sulfate concentrations, 1–3% of BC, 2–3% of CO, and 0.5–1.5% of ozone over the western contiguous United States (west of  $100^\circ\text{W}$ ). On a monthly basis, the trans-Pacific transport of Chinese air pollution was enhanced in spring (SI Appendix, Fig. S7) due to active cyclonic activities and strong westerly winds (24, 34).

The trans-Pacific transport is largely episodic (28, 35), such that the influence of Chinese pollution on US air quality varies significantly from one day to another. Fig. 3 shows the maximum contribution of EEE-related Chinese air pollution to daily mean surface air pollutant concentrations over the United States in 2006. On a day-to-day basis, the transport of EEE-related Chinese pollution contributed, at a maximum, 12–24% of sulfate

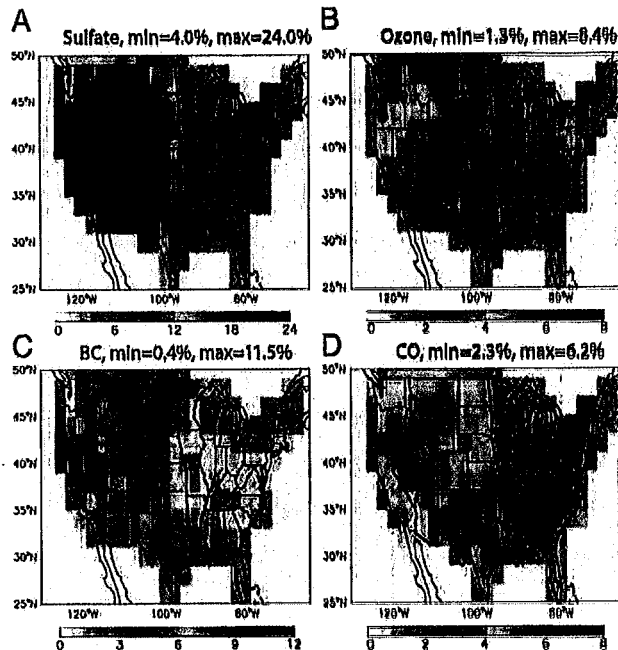
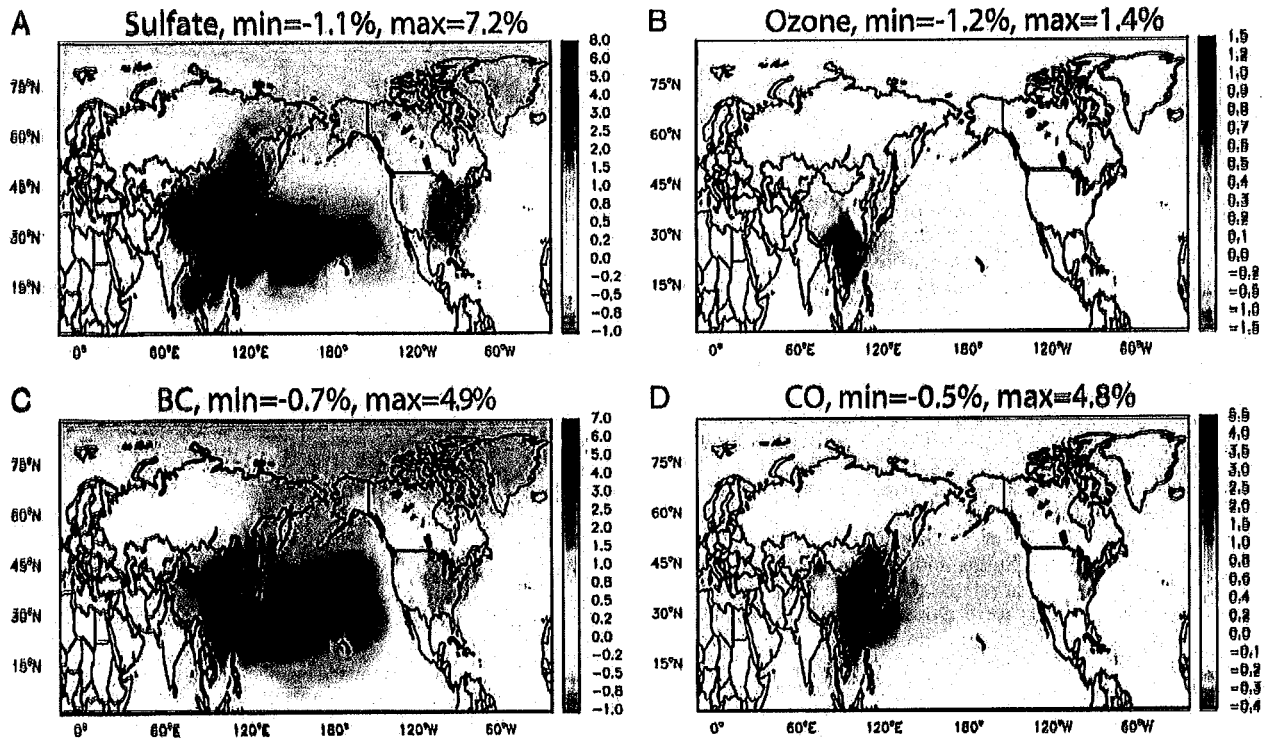


Fig. 3. Simulated maximum percentage contribution of Chinese EEE to daily mean US surface air pollution in 2006 for (A) sulfate, (B) ozone, (C) BC, and (D) CO. Results are presented as the maximum value across the 365 d in 2006 of (simulation 1 – simulation 2)/simulation 1 in SI Appendix, section 6. Results outside of the contiguous United States are colored in gray. The maximum contribution of EEE-related Chinese air pollution to US pollutant levels on a day-to-day basis is much greater than the annual mean influence.

concentrations, 2–5% of ozone, 4–6% of CO, and up to 11% of BC over the western United States; and it also contributed up to 8% of daily mean ozone over parts of the Great Lakes region. Furthermore, the trans-Pacific transport increased the number of days in 2006 when the daily maximum 8-h average ozone concentration exceeded the current US standard (75 ppb). For the 217 model gridcells constituting the contiguous United States, there are 38 gridcells that had one extra day or more of ozone exceedance in 2006 because of the transport of the EEE-related Chinese air pollution, including the gridcells covering the Los Angeles area and many regions in the eastern United States (SI Appendix, Fig. S8).

In 2006, China-to-US export of goods resulted in about 7.4% of the production-based Chinese emissions for  $\text{SO}_2$ , 5.7% for  $\text{NO}_x$ , 3.6% for BC, and 4.6% for CO. Meanwhile, outsourcing manufacture to China also led to a reduction in production-based US emissions. Had the United States produced all of the goods that are actually imported from China under a hypothetical scenario, we estimate that the production-based US emissions in 2006 would be higher by 1.7% for  $\text{SO}_2$ , 1.3% for  $\text{NO}_x$ , 0.8% for BC, and 1.1% for CO, after accounting for the difference in emission intensity between the two countries (SI Appendix, Table S1). No China-to-US exports would also mean less production-based Chinese emissions. We used GEOS-Chem to simulate the changes in 2006 surface air quality in China and the United States due to emission changes in both countries with versus without China-to-US exports, assuming the spatial variability of emissions to be unaffected. The modeling results in Fig. 4 show that about 3–7% of annual mean surface sulfate concentrations, 2–5% of BC, and 2–5% of CO over East China in 2006 were caused by the Chinese EEE due to its production of goods for US consumption. Over the eastern United States (east of  $100^\circ\text{W}$ ), annual mean surface concentrations in 2006 were



**Fig. 4.** Simulated percentage change in 2006 surface air pollution due to Chinese export of goods to the United States versus producing the same goods in the United States for (A) sulfate, (B) ozone, (C) BC, and (D) CO. Results are shown for annual mean concentrations in the lowest model layer (0–150 m), presented as (simulation 1 – simulation 6)/simulation 1 in the *SI Appendix*, section 6. The color scale is nonlinear to better present the wide range of impacts over different regions. The China-to-US export of goods results in enhanced (production-based) emissions of China with a reduction in US emissions. Air quality in China worsens as a result of these additional emissions. Over the western United States, concentrations of sulfate, ozone, and CO also increase because the elevated transport of Chinese pollution overcompensates for the effect of reduced US emissions. Meanwhile, concentrations of sulfate, BC, and CO decrease over the eastern United States, a beneficial effect particularly given its high population density.

reduced by 0.5–1.1% for sulfate, 0.5–0.8% for BC, and 0–0.5% for CO as a result of US emission reductions due to outsourcing manufacture to China. Over the western United States, however, sulfate concentrations were enhanced by 0–2% and ozone and CO levels were also increased slightly. These increases occurred because the transport of EEE-related Chinese pollution overcompensated for the effect of reduced US emissions. Given the much higher population density in the eastern United States (<http://sedac.ciesin.columbia.edu/data/collection/gpw-v3; for 2005>), outsourcing manufacture to China resulted in an overall beneficial effect for the US public health. In particular, population-weighted average sulfate, BC, and CO concentrations decreased by 0.3–0.9% over the United States (125°W–70°W, 33°N–49°N) with a negligible increase of 0.1% in ozone. This benefit, however, was at the expense of air quality deterioration over the western United States and the populous Chinese regions.

Our emission and atmospheric model results are subject to uncertainties from a variety of sources. The emission calculations are affected by errors in emission factors, economic statistics, and input–output tables. A detailed error analysis for total emissions, EEE, and BEI is presented in the *SI Appendix*, sections 3 and 5.3, based on Monte Carlo simulations. For EEE, the overall uncertainties (95% confidence intervals around the central estimates) are about –17% to 17% for SO<sub>2</sub>, –27% to 27% for NO<sub>x</sub>, –45% to 45% for CO, and –35% to 51% for BC. The uncertainties for BEI are larger for these pollutants reflecting our simplified treatment of BEI (*SI Appendix*, sections 1.1.1 and 5.3). The uncertainties for EET are close to those for EEE. The atmospheric model simulations are subject to errors in emission inputs as well as errors in the model representations

of tropospheric chemical and meteorological processes. The chemistry- and meteorology-related model uncertainties are difficult to quantify and are likely on the order of 30% (36). For the model results in Figs. 2–4 presented as percentage contribution, the uncertainties may be reduced substantially because the presented values are the normalized differences between pollutant concentrations from various model simulations (*SI Appendix*, section 6) whose uncertainties may largely offset each other. Our modeling results are for 2006, and the results may be different for other years.

### Discussion

Rising emissions produced in China are a key reason global emissions of air pollutants have remained at a high level during 2008–2009 even as emissions produced in the United States, Europe, and Japan have decreased. However, our results indicate that about 36% of SO<sub>2</sub> and 27% of NO<sub>x</sub> emitted in China in 2006 (19–24% in 2009) were related to goods exported for consumption outside of China. If all of the emissions were reallocated according to where goods are consumed (i.e., based on consumption-based accounting), emissions of many of China's trade partners would be much higher. For example, the US emissions for SO<sub>2</sub>, NO<sub>x</sub>, CO, and BC would be 6–19% higher in 2006 if the emissions embodied in its trade with China were included (Fig. 1 A–D; thick green versus thin green lines). And as we have also shown, outsourcing production to China does not always relieve consumers in the United States—or for that matter many countries in the Northern Hemisphere—from the environmental impacts of air pollution. Sulfate air quality in the western United States is poorer because of transport of Chinese

pollution associated with production of goods for US consumption, although air quality in the eastern United States is improved.

The thin purple lines in Fig. 1 E–H show the significant progress China has made since 2000, in reducing the (production-based) emissions per unit GDP through technological improvements and changes in economic structure (7, 37). In particular, SO<sub>2</sub> emissions per unit GDP are decreasing rapidly since 2004 (38) (Fig. 1E). However, the emissions per unit GDP for all pollutants remain much higher than those of the United States (Fig. 1 E–H), and further improvements in technology and economic structure could reduce emissions of pollutants much more. Differences in the ratio of pollutant to CO<sub>2</sub> emissions between the United States and China (SI Appendix, section 7 and Table S11) indicate that production-based Chinese emissions could be reduced by 58–62% for SO<sub>2</sub>, 47–54% for CO, and up to 22% for NO<sub>x</sub> over 2000–2009 if China were to enhance energy efficiency and deploy emission control technologies as effective as those used in the United States. Even if such improvements were made to only those facilities involved in producing goods for export, the reduction in emissions would significantly improve the air quality in China and in downwind regions. For instance, the annual mean surface sulfate concentrations in 2006 would have been about 10–19% lower in China and 1–5% lower in the western United States based on the simulation of GEOS-Chem.

Consideration of international cooperation to reduce transboundary transport of air pollution (31) must confront the question of who is responsible for emissions in one country during production of goods to support consumption in another. Polluting industries in China and other emerging economies supply a large proportion of global consumption through international

trade. Sustaining the current trading system while minimizing transboundary air pollution—and other environmental impacts—will likely require international agreements informed by consumption-based accounting of emissions of air pollutants as well as atmospheric transport modeling of air pollution.

## Materials and Methods

Calculation of EEE and EEI is based on an input–output analysis of the economic processes required to produce a particular good or service, multiplied by sector-specific emission intensities. See SI Appendix, Fig. S1 for the flowchart. Emissions from ocean shipping vessels are not accounted for. Sectoral emission intensities are calculated as total production-based Chinese emissions (which are estimated with a technology-based, bottom-up approach) divided by total monetary outputs from the respective sectors. The estimated production-based total emissions are consistent with the literature (SI Appendix, Fig. S3). A Monte Carlo method is used to quantify uncertainty associated with errors in emission factors, economic statistics, and the input–output analysis itself. Emissions of CO<sub>2</sub> are calculated with a similar approach, and the resulting emissions embodied in trade are consistent with previous studies (SI Appendix, Fig. S4). The global GEOS-Chem chemical transport model (version 8-03-02; on the 2.5° long × 2° lat grid) is used to simulate the impacts of EEE-related Chinese air pollution on the global atmospheric environment. We do not distinguish the EEE of volatile organic compounds that would otherwise enhance the modeled ozone production efficiency of NO<sub>x</sub>; a sensitivity simulation shows that the effect is mostly confined in the North China Plain (SI Appendix, section 6 and Fig. S6). Detailed descriptions of our analytic approach, data sources, and model simulations are presented in SI Appendix.

**ACKNOWLEDGMENTS.** We thank Michael Prather for comments. This research is supported by the National Natural Science Foundation of China, Grants 41175127, 41005078, 41222036, 21221004, 41328009, and J1103404. The work at Tsinghua University is also supported by the Tsinghua University Initiative Research Program (2011Z01026).

- Guan D, Peters GP, Weber CL, Hubacek K (2009) Journey to world top emitter: An analysis of the driving forces of China's recent CO<sub>2</sub> emissions surge. *Geophys Res Lett* 36(4):L04709.
- National Bureau of Statistics (2001–2010) *China Trade and External Economic Statistical Yearbook* (China Statistics Press, Beijing).
- Minx JC, et al. (2011) A "carbonizing dragon": China's fast growing CO<sub>2</sub> emissions revisited. *Environ Sci Technol* 45(21):9144–9153.
- Fan Y, Xia Y (2012) Exploring energy consumption and demand in China. *Energy* 40(1):23–30.
- Ohara T, et al. (2007) An Asian emission inventory of anthropogenic emission sources for the period 1980–2020. *Atmos Chem Phys* 7(16):4419–4444.
- Lu Z, Zhang Q, Streets DG (2011) Sulfur dioxide and primary carbonaceous aerosol emissions in China and India, 1996–2010. *Atmos Chem Phys* 11(18):9839–9864.
- Lin J, et al. (2010) Recent changes in particulate air pollution over China observed from space and the ground: Effectiveness of emission control. *Environ Sci Technol* 44(20):7771–7776.
- Zhang Q, He KB, Huo H (2012) Policy: Cleaning China's air. *Nature* 484(7393):161–162.
- Peters GP, Minx JC, Weber CL, Edenhofer O (2011) Growth in emission transfers via international trade from 1990 to 2008. *Proc Natl Acad Sci USA* 108(21):8903–8908.
- Davis SJ, Caldeira K (2010) Consumption-based accounting of CO<sub>2</sub> emissions. *Proc Natl Acad Sci USA* 107(12):5067–5072.
- Hertwich EG, Peters GP (2009) Carbon footprint of nations: A global, trade-linked analysis. *Environ Sci Technol* 43(16):8414–8420.
- Peters GP, Hertwich EG (2008) CO<sub>2</sub> embodied in international trade with implications for global climate policy. *Environ Sci Technol* 42(5):1401–1407.
- Janssens-Maenhout G, Petrascu AMN, Muntean M, Blujdea V (2010) *Verifying Greenhouse Gas Emissions: Methods to Support International Climate Agreements* (The National Academies Press, Atlanta).
- Streets DG, Yu C, Bergin MH, Wang XM, Carmichael GR (2006) Modelling study of air pollution due to the manufacture of export goods in China's Pearl River Delta. *Environ Sci Technol* 40(7):2099–2107.
- Smith KR, et al. (2009) Public health benefits of strategies to reduce greenhouse-gas emissions: Health implications of short-lived greenhouse pollutants. *Lancet* 374(9707):2091–2103.
- Becker DW, et al. (1993) An association between air pollution and mortality in six U.S. cities. *N Engl J Med* 329(24):1793–1799.
- Pope CA, 3rd, et al. (2002) Lung cancer, cardiopulmonary mortality, and long-term exposure to fine particulate air pollution. *JAMA* 287(9):1132–1141.
- Bell ML, Dominici P, Samet JM (2005) A meta-analysis of time-series studies of ozone and mortality with comparison to the national morbidity, mortality, and air pollution study. *Epidemiology* 16(4):436–445.
- Van Dingenen R, et al. (2009) The global impact of ozone on agricultural crop yields under current and future air quality legislation. *Atmos Environ* 43:604–618.
- Wittig VE, Alnsworth EA, Naidu SL, Karnosky DF, Long SP (2009) Quantifying the impact of current and future tropospheric ozone on tree biomass, growth, physiology and biochemistry: A quantitative meta-analysis. *Glob Change Biol* 15(2):386–424.
- Ramanathan V, Carmichael G (2008) Global and regional climate changes due to black carbon. *Nat Geosci* 1(4):221–227.
- Penner JE, et al. (2010) Short-lived uncertainty? *Nat Geosci* 3(9):507–508.
- Jaffe D, et al. (1999) Transport of Asian air pollution to North America. *Geophys Res Lett* 26(6):711–714.
- Zhang L, et al. (2008) Transpacific transport of ozone pollution and the effect of recent Asian emission increases on air quality in North America: An integrated analysis using satellite, aircraft, ozonesonde, and surface observations. *Atmos Chem Phys* 8(20):6117–6136.
- Fioré AM, et al. (2002) Background ozone over the United States in summer: Origin, trend, and contribution to pollution episodes. *J Geophys Res, D, Atmospheres* 107(D15):4275.
- Cooper OR, et al. (2010) Increasing springtime ozone mixing ratios in the free troposphere over western North America. *Nature* 463(7279):344–346.
- Yu H, et al. (2012) Aerosols from overseas rival domestic emissions over North America. *Science* 337(6094):566–569.
- Wuebbles DJ, Lei H, Lin JT (2007) Intercontinental transport of aerosols and photochemical oxidants from Asia and its consequences. *Environ Pollut* 150(1):65–84.
- Lin JT, Wuebbles DJ, Liang XZ (2008) Effects of intercontinental transport on surface ozone over the United States: Present and future assessment with a global model. *Geophys Res Lett* 35(2):L02805.
- Shue H (1999) Global Environment and International Inequality. *Int Aff* 75(3):531–545.
- HTAP Task Force (2010) *Hemispheric Transport of Air Pollution 2010 Executive Summary* (Convention on Long-Range Transboundary Air Pollution, Geneva).
- Weber CL, Matthews HS (2007) Embodied environmental emissions in U.S. international trade, 1997–2004. *Environ Sci Technol* 41(14):4875–4881.
- Selinfeld JH, Pandis SN (2006) *Atmospheric Chemistry and Physics: From Air Pollution to Climate Change* (Wiley, Hoboken, NJ), 2nd Ed.
- Jacob DJ, et al. (2003) Transport and chemical evolution over the Pacific (TRACE-P) aircraft mission: Design, execution, and first results. *J. Geophys. Res.* 108(D20)(9000).
- Ylanger JJ, et al. (2000) The episodic nature of air pollution transport from Asia to North America. *J Geophys Res, D, Atmospheres* 105(D22):26931–26945.
- Lin JT, et al. (2012) Modeling uncertainties for tropospheric nitrogen dioxide columns affecting satellite-based inverse modeling of nitrogen oxides emissions. *Atmos Chem Phys* 12(24):12255–12275.
- National Bureau of Statistics (2001–2010) *China Statistical Yearbook* (China Statistics Press, Beijing).
- Xu Y (2011) Improvements in the operation of SO<sub>2</sub> scrubbers in China's coal power plants. *Environ Sci Technol* 45(2):380–385.

Opinion

**Share Access View**

You are viewing the full text of this article because it was shared by a San Francisco Chronicle subscriber.

Subscribe today for full access to the San Francisco Chronicle in print, online and on your iPad.

Subscribe

# Keep coal out of Oakland port

By Loni Hancock, Rob Bonta and Tony Thurmond | July 20, 2015 | Updated: July 20, 2015 3:39pm